

SOURCE APPORTIONMENT STUDY FOR STRUGA URBAN AREA



GOCE DELCEV
UNIVERSITY
FACULTY OF NATURAL
AND TECHNICAL SCIENCES

AMBICON.UGD

This study was prepared by the AMBICON laboratory at Goce Delcev University—Stip as part of the "Scaling-up Actions to Tackle Air Pollution" project, which is implemented by the United Nations Development Programme (UNDP) in partnership with the Ministry of Environment and Physical Planning, along with the municipalities of Kavadarci, Kumanovo, Gostivar, Struga, and Strumica.

The project is a component of the UNDP Framework Programme funded by Sweden. The Programme also includes the project "Building municipal capacities for project implementation".

The views expressed in this study are those of the author and do not necessarily reflect the views of the UNDP, Sweden as the donor, or the other project partners.

Document title:	Source Apportionment Study for Struga urban area
Name of the organization:	University Goce Delcev, Stip, AMBICON Lab – Faculty of Natural and Technical Sciences
Country	Republic of North Macedonia
Project title:	Scaling-up actions to tackle air pollution
Project Number:	00122883
Submitted To:	UNDP, Skopje
Date of submission	03.04.2025
Project team	
Team leader	Prof. Dr. Dejan Mirakovski – UGD FNTS
Chemical speciation and modelling	Ass. Prof. Dr. Afrodita Zendelska – UGD FNTS
QA/QC group	Prof. Dr. Marija Hadzi-Nikolova – UGD FNTS Prof. Dr. Blazo Boev – UGD FNTS
Laboratory process support	Prof. Dr. Tena Sijakova-Ivanova – UGD FNTS Ass. Prof. Dr. Ivan Boev – UGD FNTS Prof. Dr. Sonja Lepitkova – UGD FNTS Ass. Prof. Dr. Gorgi Dimov – UGD FNTS Ass. M.Sc. Ana Mihailovska – UGD FNTS
Technical group	M.Sc. Boban Samardziski, FNTS, AMBICON Igor Pavlov – FNTS, AMBICON Goce Bogatinov – UGD IT SG
Students' internship	Ana Marija Kostadinova
UNDP	Armen Grigoryan, Resident Representative Aleksandra Dimova Manchevska, Project Manager Dren Nevzati, Monitoring Associate Trajancho Naumovski, Project Assistant
Knowledge management and capacity building support	M.Sc. Pavlina Zdraveva
Communication support team	Igor Stojanov Elena Doneva

Contents

List of figures.....	4
List of tables.....	5
Symbols and abbreviations.....	5
Terms and definitions	6
1. Introduction	8
2. Background information's	9
2.1. Struga urban area	9
2.2. Climate	10
2.3. Transportation and energy infrastructure	11
2.4. Industry and service providers.....	12
2.5. Historical data on ambient air quality	13
3. Major emission sources.....	13
3.1. Emission inventory	13
3.2. Source profiles	14
4. Particulate matter sampling and analysis	19
4.1. Sampling and determination of mass concentration of ambient particulate matter (PM2.5) 19	
4.2. Chemical speciation.....	22
4.3. Observations and results	26
Statistical Evaluation	26
5. Positive Matrix Factorisation	33
5.1. Input data and PMF model setting	35
5.2. Factor attribution to sources	35
5.3. Sources Contribution.....	40
6. Conclusions and recommendations	43
Lessons learned.....	45
References.....	46

List of figures

Figure 1. Map of municipalities included in this study	8
Figure 2. Location of Municipalities of Struga	9
Figure 3. Struga topography map [2].....	10
Figure 4. Maximum and minimum temperature maps for North Macedonia with probability of occurrence of 0,002% (Source: Climate maps, UHMR, 2020).....	10
Figure 5. Seasonal wind roses during the monitoring period (March 2023 to February 2024, AMBICON Lab).....	11
Figure 6. Number of registered vehicles in Struga classified according to the type and fuel used	12
Figure 7. Spatial distribution of industrial/production plants, commercial and public service provider in the municipality of Struga [1]	13
Figure 10. Sectoral contribution to particulate mater emissions	14
Figure 11. Woodstove burning chemical profile (closed fireplace).....	15
Figure 12. Open burning of crop residues chemical profile.....	15
Figure 13. Construction activities chemical profile	16
Figure 14. Exhaust diesel and gasoline chemical profile	16
Figure 15. Urban traffic chemical profile	16
Figure 16. Road dust chemical profile	17
Figure 17. Soil dust chemical profile	17
Figure 18. Residual oil chemical profile.....	18
Figure 19. Fuel oil chemical profile	18
Figure 20. Monitoring location in Struga urban area	19
Figure 21. Sequential sampling system PNS 18T-DM 6.1.....	20
Figure 22. Weighing room- AMBICON UGD Lab	21
Figure 23. NEX CG by Rigaku.....	23
Figure 24. Spectroquant® Prove 600, Merck.....	25
Figure 25. Magee Scientific, SootScan™ Model OT21 Optical Transmissometer	26
Figure 26. PM 2.5 – daily average concentrations from March 2023 to March 2024	29
Figure 27. Daily variations in concentrations throughout all days, seasons, and weekdays	30
Figure 28. Bi-variate (seasonal), CPF and non parametric polar plots	30
Figure 29. Major components and elemental groups identified	31
Figure 30. Contribution of major particulate matter components [20, 21]	32
Figure 31. Average monthly concentrations of lead (Pb) and nickel (Ni) in Struga	32
Figure 32. Free software US-EPA PMF 5.0 version 5.0.14 – splash screen	34
Figure 33. Factor fingerprint for Struga	36
Figure 34. Biomass burning factor profiles in Struga	36
Figure 35. Traffic associated factors for Struga dataset.....	37
Figure 36. Fuel and residual oil factor profiles	38
Figure 37. Mineral dust factor profiles	39
Figure 38. Open fire burning factor profile	39
Figure 39. Secondary Aerosols factor profile	40
Figure 40. Average monthly contributions to total particulate mass (PM 2.5) – Struga	40
Figure 41. Relative monthly contribution – Struga	41
Figure 42. Relative annual contribution of PM 2.5 sources at Struga	42

List of tables

Table 1. Criteria pollutants emissions (in tons per year) for Struga municipality [1]	14
Table 2. Quality control results of EDXRF NEX CG by Rigaku	23
Table 3. Zeta-score results of EDXRF inter-laboratory comparison	24
Table 4. Quality control results for water soluble ions standard operating procedure.....	25
Table 5. Statistical evaluation – Struga dataset.....	27
Table 6. Corelation matrix – Struga dataset	28

Symbols and abbreviations

For the purposes of this document, the following symbols and abbreviated terms apply.

- C Concentration of PM ($\mu\text{g}/\text{m}^3$) at ambient conditions
- GUM Guide to the Expression of Uncertainty in Measurement
- JCGM Joint Committee for Guides in Metrology
- PM Particulate Matter
- PTFE Polytetrafluoroethylene
- QA/QC Quality Assurance / Quality Control
- NIST National Institute of Standards and Technology
- QCS Quality Control Sample
- AQIP Academic Quality Improvement Plan
- EEA European Environment Agency
- TSP Total suspended particles
- NMVOC Non-methane volatile organic compounds
- MOEPP Ministry of environment and physical planning
- ED-XRF Energy dispersive X-ray fluorescence
- IC Ion chromatography
- OC Organic carbon
- EC Elemental carbon
- SA Source apportionment
- SD Standard deviation
- C.V. Coefficient of variation

Terms and definitions

For the purposes of this document, the following terms and definitions apply.

Ambient air – is outdoor air in the troposphere, excluding workplaces as defined by Directive 89/654/EEC [12] where provisions concerning health and safety at work apply and to which members of the public do not have regular access.

Calibration - operation that, under specified conditions, in a first step, establishes a relation between the quantity values with measurement uncertainties provided by measurement standards and corresponding indications with associated measurement uncertainties and, in a second step, uses this information to establish a relation for obtaining a measurement result from an indication.

Calibration Standard (CAL) - a solution prepared from the stock standard solution(s) which is used to calibrate the instrument response with respect to analyte concentration.

Certified reference material (CRM) is defined as a “reference material characterized by a metrologically valid procedure for one or more specified properties, accompanied by a reference material certificate that provides the value of the specified property, its associated uncertainty, and a statement of metrological traceability”.

Combined standard uncertainty - standard uncertainty of the result of a measurement when that result is obtained from the values of a number of other quantities, equal to the positive square root of a sum of terms, the terms being the variances or covariances of these other quantities weighted according to how the measurement result varies with changes in these quantities.

Coverage factor - numerical factor used as a multiplier of the combined standard uncertainty in order to obtain an expanded uncertainty.

Expanded uncertainty - quantity defining an interval about the result of a measurement that may be expected to encompass a large fraction of the distribution of values that could reasonably be attributed to the measurand.

Field blank - filter that undergoes the same procedures of conditioning and weighing as a sample filter, including transport to and from, and storage in the field, but is not used for sampling air, and it has the same treatment as samples.

Instrument Detection Limit (IDL) - the concentration equivalent of the analyte signal, which is equal to three times the standard deviation of the blank signal at the selected analytical mass(es).

Internal Standard - pure analyte(s) added to a solution in known amount(s) and used to measure the relative responses of other method analytes that are components of the same solution. The internal standard must be an analyte that is not a sample component.

Laboratory Reagent Blank (LRB) (Preparation Blank) - an aliquot of reagent water that is treated exactly as a sample including exposure to all labware, equipment, solvents, reagents, and internal standards that are used with other samples. The LRB is used to determine if method analytes or other interferences are present in the laboratory environment, the reagents or apparatus.

Linear Dynamic Range (LDR) - the concentration range over which the analytical working curve remains linear.

Limit value - level fixed based on scientific knowledge, with the aim of avoiding, preventing or reducing harmful effects on human health and/or the environment, to be attained within a given period and not to be exceeded once attained.

Method Detection Limit (MDL) - the minimum concentration of an analyte that can be identified, measured and reported with 99% confidence that the analyte concentration is greater than zero. MDLs are intended as a guide to instrumental limits typical of a system optimized for multi-element determinations and employing commercial instrumentation and pneumatic nebulization sample introduction. However, actual MDLs and linear working ranges will be dependent on the sample matrix, instrumentation and selected operating conditions.

Performance characteristic - one of the parameters assigned to a sampler to define its performance.

Performance criterion - limiting quantitative numerical value assigned to a performance characteristic, to which conformance is tested.

Period of unattended operation - time over which the sampler can be operated without requiring operator intervention.

PM_x - particulate matter suspended in air which is small enough to pass through a size-selective inlet with a 50 % efficiency cut-off at $x \mu\text{m}$ aerodynamic diameter.

Quality Control Sample (QCS) - a solution containing known concentrations of method analytes which is used to fortify an aliquot of LRB matrix. The QCS is obtained from a source external to the laboratory and is used to check laboratory performance.

Reference method (RM) - measurement method(ology) which, by convention, gives the accepted reference value of the measurand.

Sampled air - ambient air that has been sampled through the sampling inlet and sampling system.

Sampling inlet - entrance to the sampling system where ambient air is collected from the atmosphere.

Standard uncertainty - uncertainty of the result of a measurement expressed as a standard deviation.

Stock Standards Solutions - a concentrated solution containing one or more analytes prepared in the laboratory using assayed reference compounds or purchased from a reputable commercial source.

Suspended particulate matter - notion of all particles surrounded by air in a given, undisturbed volume of air.

Tuning Solution - a solution used to determine acceptable instrument performance prior to calibration and sample analyses.

Time coverage - percentage of the reference period of the relevant limit value for which valid data for aggregation have been collected.

Uncertainty (of measurement) - parameter associated with the result of a measurement that characterizes the dispersion of the values that could reasonably be attributed to the measurand

Weighing room blank - filter that undergoes the same procedures of conditioning and weighing as a sample filter, but is stored in the weighing room

1. Introduction

The "Scaling-up actions to tackle air pollution" project is a component of the UNDP Framework Programme, funded by Sweden. The project is being executed in North Macedonia by the United Nations Development Program (UNDP), in partnership with the Ministry of Environment and Physical Planning, as well as the municipalities of Gostivar, Kavadarci, Kumanovo, Struga, and Strumica.

Building on the results and lessons learned from the first phase conducted in Skopje, the project aims to scale up and replicate the developed concept in five additional cities facing air pollution challenges: Gostivar, Kavadarci, Kumanovo, Struga, and Strumica. Following the successful completion of the Source Apportionment Study for the City of Skopje, the AMBICON Laboratory has been tasked with preparing the Source Apportionment Studies for the five new municipalities: Gostivar, Kavadarci, Kumanovo, Struga, and Strumica.

The primary objective of a source apportionment study is to collect insights regarding pollution sources and their contributions to ambient air pollution levels. This information is essential for developing effective air quality policies, which are necessary for the implementation of the Air Quality Directives (Directive 2008/50/EC and Directive 2004/107/EC).

The actions undertaken followed the rigorous study approach outlined in the European guide on air pollution source apportionment with receptor models (Revised edition 2019, JRC) and included:

- Preliminary evaluation of areas under examination (emission inventories, time series of pollutants and meteorology etc),
- Selection of representative receptors/monitoring sites,
- Sampling and chemical speciation,
- Construction of multivariate receptor model.

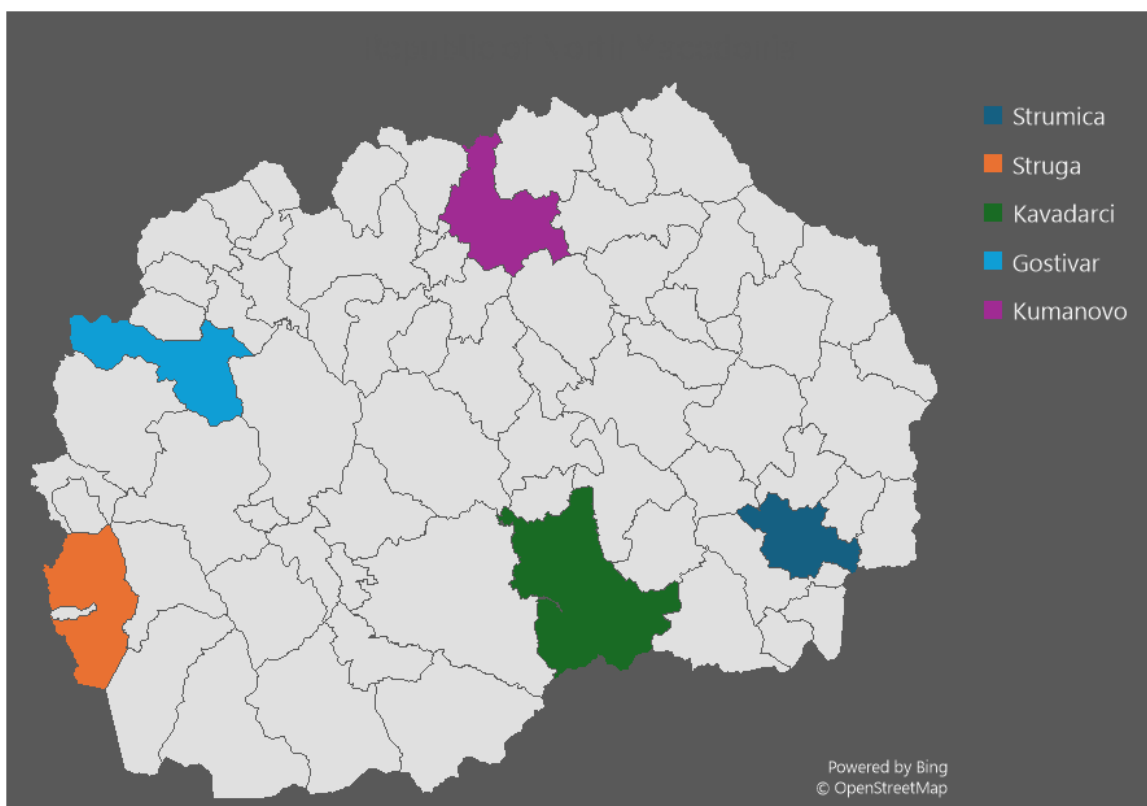


Figure 1. Map of municipalities included in this study

The project also included an indoor air quality study for ten selected public buildings—kindergartens and schools—across the urban areas of five pilot municipalities. The study aimed to assess the current air quality and develop strategies for creating a healthier indoor environment in these facilities.

This research represents one of the first efforts to provide quantitative information on the contributions of various pollution sources to ambient PM2.5 levels in urban centers outside the capital city's urban area. Consequently, the research produced a unique data set that could be used to improve air quality by addressing strategies for mitigating air pollution and implementing effective air protection measures.

2. Background information's

2.1. Struga urban area

The Municipality of Struga is located in the southwestern region of the Republic of North Macedonia, positioned on the northern shore of Lake Ohrid, near the point of discharge of the Crn Drim River from the lake.

The municipality covers the northwestern section of the Ohrid-Struga Valley and has a total area of 483 km². The urban area is situated on a flat terrain with an average elevation of 696 meters and spans both banks of the Crn Drim River.

According to the 2021 Census, Struga had a total population of 50980, with 14606 households and 22668 apartments and houses.

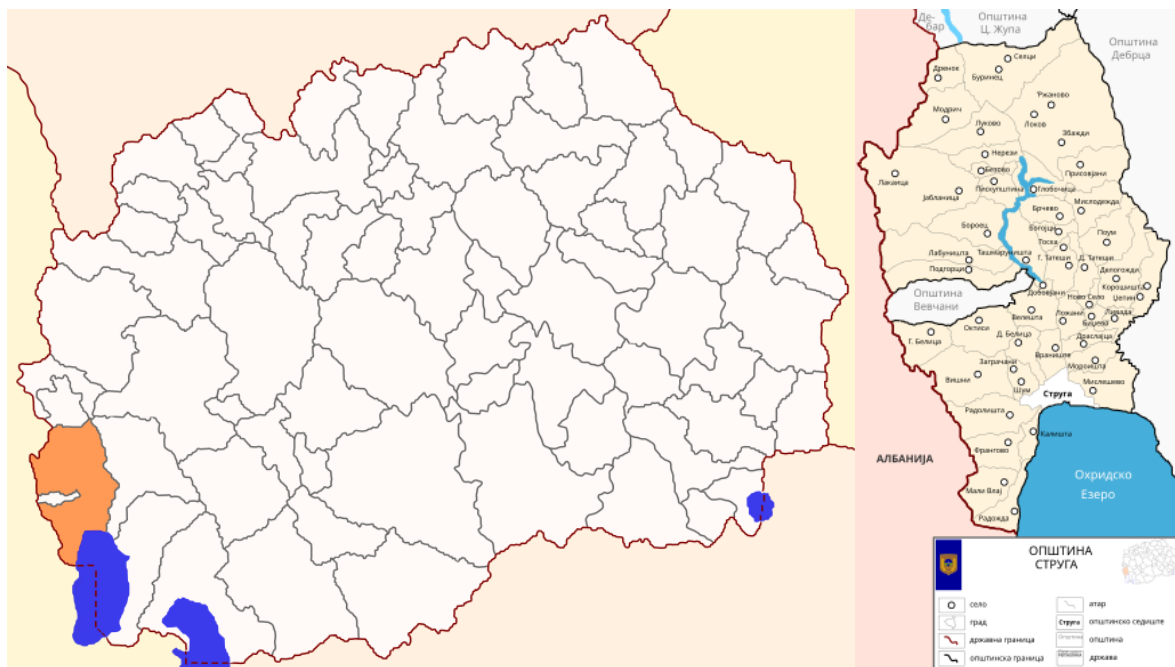


Figure 2. Location of Municipalities of Struga

The municipalities of Ohrid, Struga, and Debarca constitute a protected site of natural and cultural heritage that has been inscribed on the UNESCO World Heritage List since 2014.

Within the Municipality of Struga, a total of 85 sites have been recognized as cultural heritage objects, including 2 that hold strict protection status.

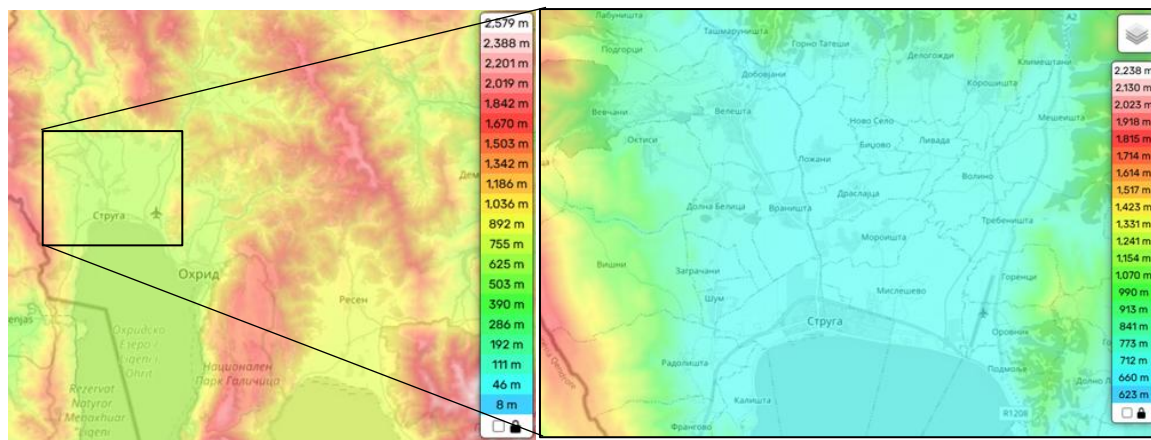


Figure 3. Struga topography map [2]

The Municipality of Struga is the only area in the country that is part of the Adriatic River Basin, and includes the catchment basins of Lake Ohrid and Lake Prespa. The principal river in this catchment area is the Crn Drim River, which originates from Lake Ohrid. On Macedonian soil, the 56-kilometer-long Crn Drim River flows into the Bel Drim River on the Republic of Albania soil, which flows into the Adriatic Sea [1].

The Struga coastline begins from the confluence of the Sateska River with Lake Ohrid and extends to the Kjafasan border crossing with the Republic of Albania. The wide valley is surrounded by steep mountains: Jablanica to the west, Karaorman and Stogovo to the north, and Galicica to the east.

2.2. Climate

The climate in the municipality of Struga is warm-continental with pronounced influences from the Adriatic Sea that penetrate along the course of the Crn Drim River, which due to the high mountains of Galicica, Karaorman and Jablanica are limited to the Ohrid-Struga Valley. The average annual temperature is 10.9 °C. The coldest month is January, and the warmest months are July and August when the temperature varies from 28 °C to 33 °C.

The average amount of precipitation in the municipality of Struga is 812 mm. There are 96 rainy days on average per year. The municipality of Struga is characterized by an average of 2208 sunny hours per year.

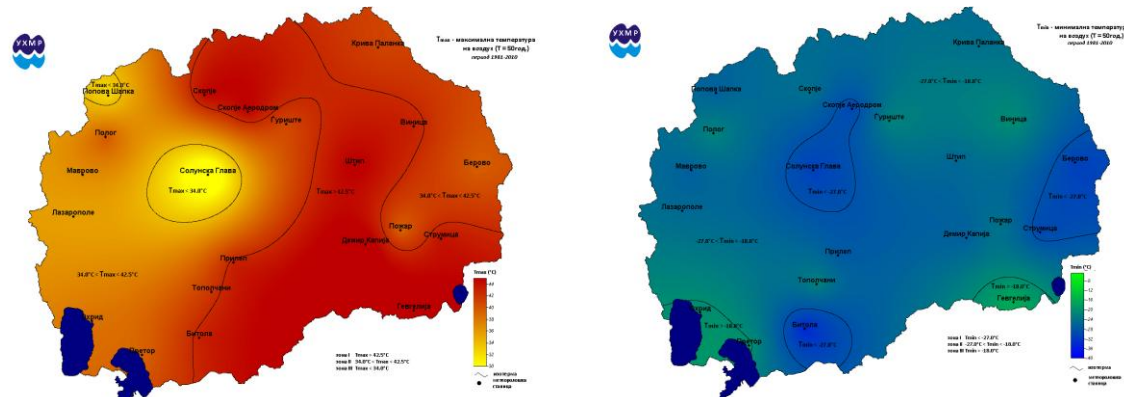


Figure 4. Maximum and minimum temperature maps for North Macedonia with probability of occurrence of 0,002% [3]

Permanent and local winds blow from different directions on the territory of the municipality of Struga. Permanent winds blow from the north and south. Winds from the north are most common in winter, but they are also present throughout the year. These winds blow along the valley of the Black Drim River and are cold winds. The winds from the south occur in the months of March and April. In Struga, the influence of the local wind Strmec is also felt, which blows from the surrounding mountains towards Lake Ohrid in the eternal hours until sunrise [1].

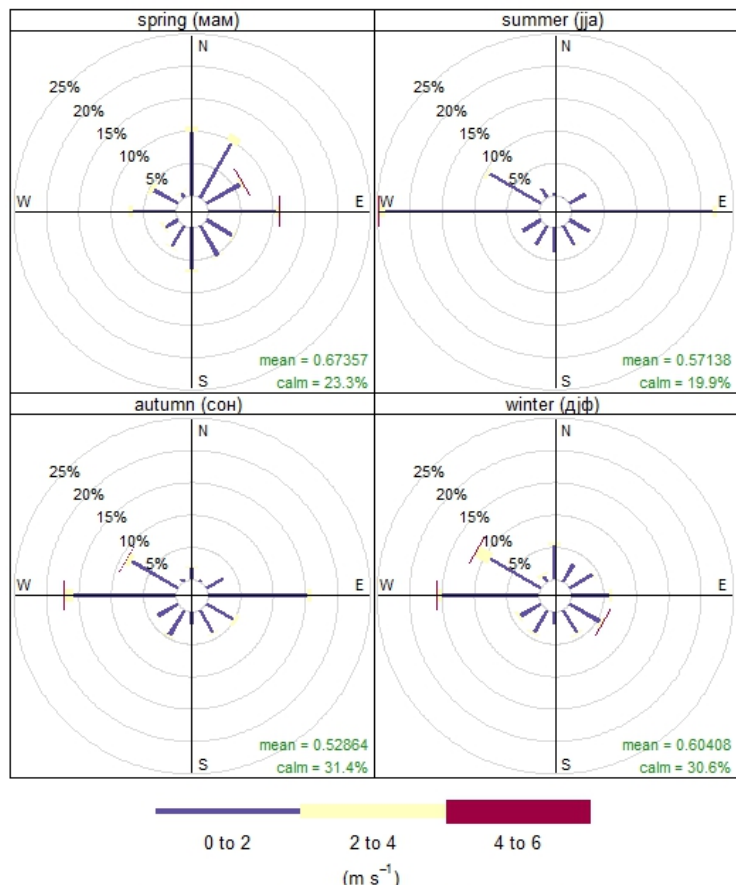


Figure 5. Seasonal wind roses during the monitoring period (March 2023 to February 2024, AMBICON Lab).

The majority of winds observed during the monitoring period show low to moderate speeds, remaining below 2 m/s. Winds with higher velocities (2 to 4 m/s) are infrequent, occurring approximately 5% of the time, while winds exceeding 4 m/s appear only sporadically.

The predominant winds in spring come from the north, east, and south, exhibiting low to moderate speeds. Summer is characterized by low-speed winds originating from the northeast and south. Autumn and winter show the longest calm periods, accounting for up to 31% of the time; however, these seasons also experience stronger winds primarily from the west/northwest and east/northeast directions.

2.3. Transportation and energy infrastructure

The territory of the Municipality of Struga features a well-developed road network that connects it to the neighboring cities of Ohrid and Debar, as well as to the rest of the country. Additionally, the Kjafasan border crossing with the Republic of Albania is situated within the municipality's territory.

The A2 expressway, which is part of the M4 Skopje-Kicevo-Ohrid highway, runs through Struga and leads to the Kjafasan border crossing with Albania.

In close proximity to the city of Struga, along the Struga-Kicevo-Skopje highway, is the "St. Paul the Apostle" airport, providing a significant link for the municipality in terms of international air transport.

In 2023, Struga recorded a record high of 19,181 vehicles, compared to 16,420 in 2021. This figure represents the count of various types of vehicles registered in Struga from 2021 to 2023, along with a classification of the vehicle fleet based on the types of fuels used [4].

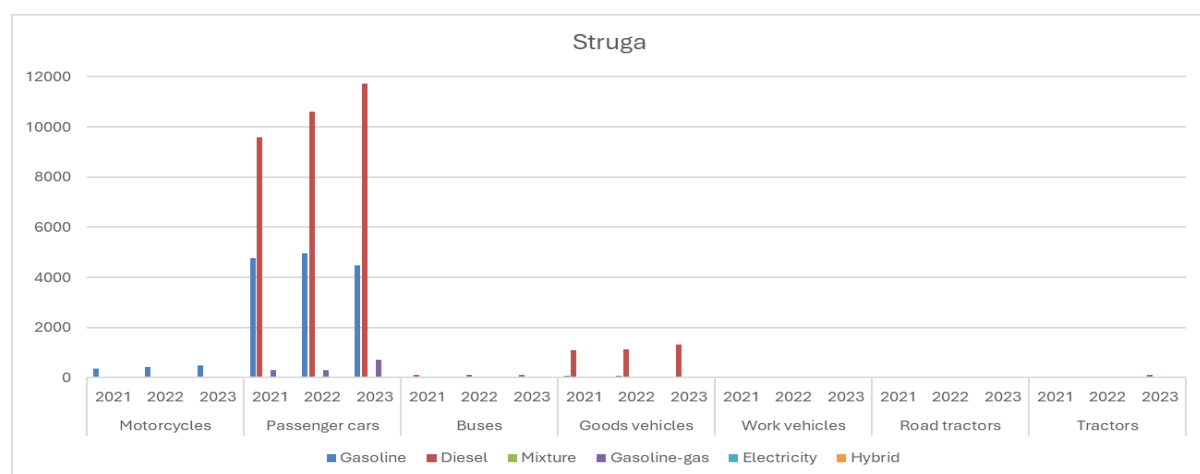


Figure 6. Number of registered vehicles in Struga classified according to the type and fuel used

The electric power is provided via a national power grid featuring a comprehensive network that encompasses the municipalities of Debar, Vevchani, Centar Župa, and portions of Mavrovo and Rostuše. This infrastructure guarantees dependable electricity access for residential and commercial users in these regions. In the urban regions of Struga and Debar, the distribution is predominantly cable-based, whereas the other areas are supplied with electricity through overhead lines.

The hydropower potential of the Crn Drim River has been utilized via the establishment of the Crn Drim hydropower system, comprising two dams and hydroelectric power plants: HPP Globocica – Struga and HPP Štipje – Debar. The Štipje hydroelectric power plant possesses an installed capacity of 84 MW and an average annual electricity production of 272 GWh, whereas the Globocica hydroelectric power plant has a height of 94.5 m, an installed capacity of 42 MW, and an average annual production of 180 GWh.

2.4. Industry and service providers

Data from the Ministry of Environment and Physical Planning and the Municipality of Struga indicate that one facility possesses an A integrated environmental permit (Ilinden AD Struga, which includes two asphalt and two concrete bases) [5], while several facilities hold a B integrated environmental permit [6].

The majority of these facilities consist of quarries and premix concrete plants that do not report significant point sources of emissions and are primarily located well outside urban areas.

Commercial and public service providers that operate small or medium combustion plants primarily for heating purposes can also significantly affect urban air quality, as many utilize outdated units fuelled by fuel or residual oil, and in some instances, solid fuels such as lignite or wood.

Most of the commercial and public service providers (schools, kindergartens, administrative and medical care facilities) are all located inside the boundaries of the urban area (see Figure 7).

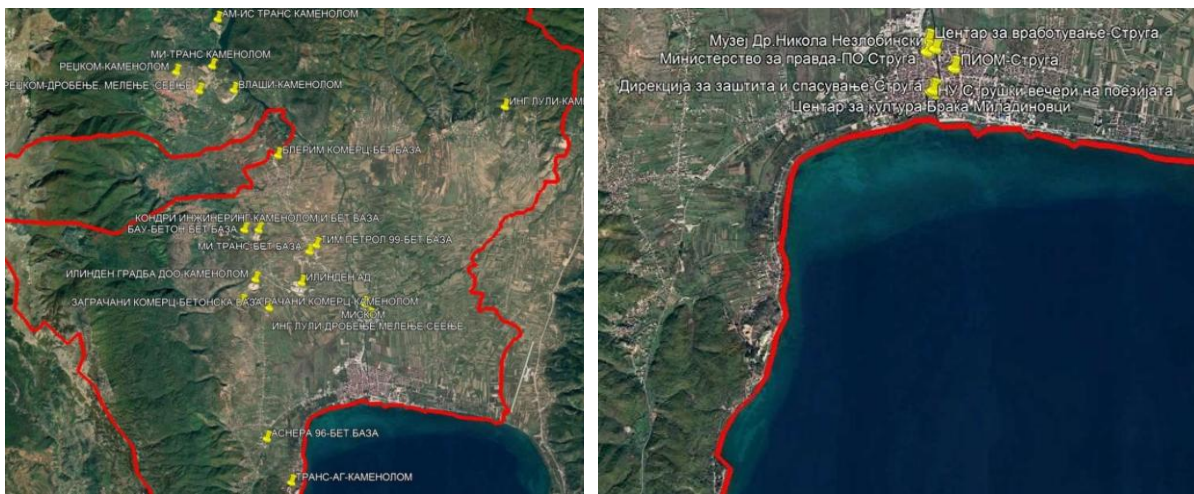


Figure 7. Spatial distribution of industrial/production plants, commercial and public service provider in the municipality of Struga [1]

2.5. Historical data on ambient air quality

The Struga urban area is not covered with the national monitoring network, and no other program has monitored ambient air quality there, so there is no historical data.

However, due to poor waste management practices and frequent landfill fires, ambient air quality has become a recognized and openly discussed issue.

Therefore, the UNDP and AMBICON Laboratory, with joint efforts, have established a permanent PM 2.5 monitoring station as part of this project, making the data publicly accessible through the cistvozduh.mk portal.

3. Major emission sources

Emission data and corresponding source profiles were compiled using several relevant sources, including the Struga Municipality Air Quality Improvement Plan for 2023-2027 [1], as well as the SPECIEUROPE repository [10], which contains chemical profiles of particulate matter obtained from source measurements conducted across Europe.

3.1. Emission inventory

The emissions inventory has been developed within the Air Quality Improvement Plan [1] by utilizing standardized approaches to estimate air pollutants and greenhouse gas (GHG) emissions across various sectors. Emissions inventories require activity data (e.g., fuel consumption, industrial output) and emission factors that indicate quantity of pollutants released per unit of activity. Data sources commonly include industrial output reports, energy statistics, transportation statistics (vehicle types and usage, fuel consumption), agricultural activities and waste management data. In this particular instance, the primary data sources were official reports from IPPC installations (MOEPP) and the MAKSTAT database (State Statistical Office) [1].

Calculations conducted follow recommended procedures based on the:

- Intergovernmental Panel on Climate Change (IPCC) Guidelines for greenhouse gas emissions.
- European Environment Agency (EEA) EMEP/EEA Air Pollutant Emission Inventory Guidebook – pertaining to air pollutants [11].

Emissions were assessed using the Tier 1 or basic approach, utilizing default emission factors from international sources according to this formula:

$$\text{Emissions} = \text{Activity Data} \times \text{Emission Factor}$$

where:

- Activity Data denotes the quantity of a particular activity (e.g., fuel consumed in tons).
- Emission Factor denotes emissions per unit of activity (e.g., kg of PM 2.5 per ton of fuel combusted).

In accordance with national regulations and guidelines (Nomenclature For Reporting - NFR and Guidelines for Drafting AQIP) [55], this inventory categorizes emissions into the following sectors: industry, transportation, public sector (administration and services), residential sector (households), industrial processes and products consumption, agriculture (which includes livestock and fertilizer usage), waste management (including emissions from landfills, wastewater treatment, and waste incineration) and natural sources.

The annual emissions of criteria pollutants have been calculated [1] and are detailed in Table 1.

Table 1. Criteria pollutants emissions (in tons per year) for Struga municipality [1]

	Pollutants (t/year)							
	NOx	CO	NMVOC	SOx	NH3	TSP	PM10	PM2.5
Industrial process	220.87	19.26	121.07	3.37	/	102.22	39.22	4.04
Administrative facilities	0.24	0.48	0.24	0.06	0.03	0.14	0.13	0.13
Households	11,90	908.12	136.07	3.24	15.85	181.83	172.26	167.73
Traffic	307.31	156.23	27.46	2.19	2.44	22.30	18.05	14.36
Waste	0.82	14.38	57.01	0.03	/	1.22	1.17	1.08
Agriculture	19.78	/	38.62	/	92.16	15.92	4.22	1.29

As illustrated above, household heating is by far most importnat source of particulate matter emissions, accounting for 73% of PM10 emissions and 89% of PM2.5 emissions.

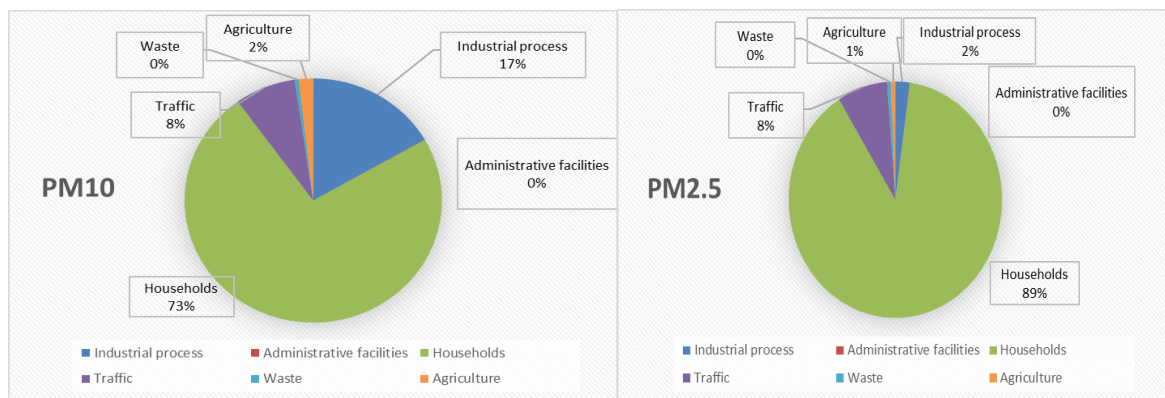


Figure 8. Sectoral contribution to particulate mater emissions

3.2. Source profiles

Chemical profiles of the sources identified in the inventory were obtained using the data published in SPECIEUROPE, a repository of source profiles developed by the JRC in the framework of FAIRMODE project [13]. SPECIEUROPE comprises chemical profiles of particulate matter, both organic and inorganic, derived from measurements of European sources and source apportionment investigations conducted in Europe.

Based on data given in the emission inventories, chemical profiles for following sources are included:

- Woodstove burning
- Open burning of crop residues

- Construction
- Traffic urban + Vehicle Exhaust
- Soil dust + Road dust
- De-icing Salt
- Fuel oil + Residual oil

A brief description of the source, sampling and analytical procedures that were employed, geographical location, elemental composition (relative mass of the elements), and bibliography are provided in the sections that follow.

Woodstove burning profile is based on JRC data, referencing closed fireplace wood combustion in Krakow, Poland. Elemental analysis was performed using particle induced x-ray emission (PIXE), photometric and ion chromatography (IC) methods are used for water soluble ions analysis, thermal optical analysis (TOT) was used for OC and EC analysis, and gas chromatography-mass spectrometry (GC-MS) for organic compounds. Organic carbon (OC) and elemental carbon (EC) are by far most abundant compounds (89.63 and 6.65 % respectively), followed by K (1.11 %) and Cl (0.43 %). Sulphates (0.87 %) and nitrates (0.25 %) are most abundant ions.

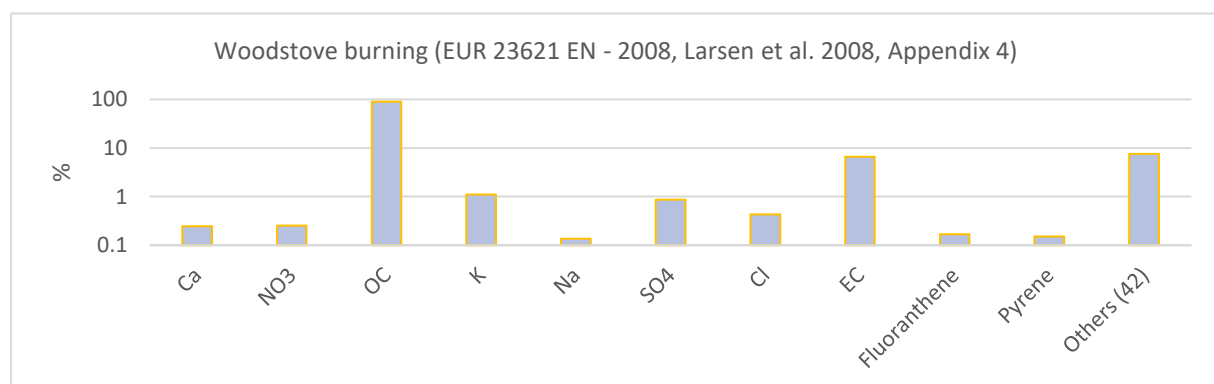


Figure 9. Woodstove burning chemical profile (closed fireplace)

Open burning of crop residues, or agricultural fields burning profile is based on direct on filter samples from Thessaloniki area in Northern Greece. Samples were analysed using energy dispersive X-ray fluorescence (ED-XRF) for elemental composition and ion chromatography (IC) for water soluble ions analysis. Bromine is most abundant element (9.43 %), followed by EC (9.0 %) and Co (9.0 %). Other metals including V (8.133 %), Ti (4.83 %) and As (1.1 %) also have significant concentrations. Sulphates (8.13 %) are by far most abundant ion.

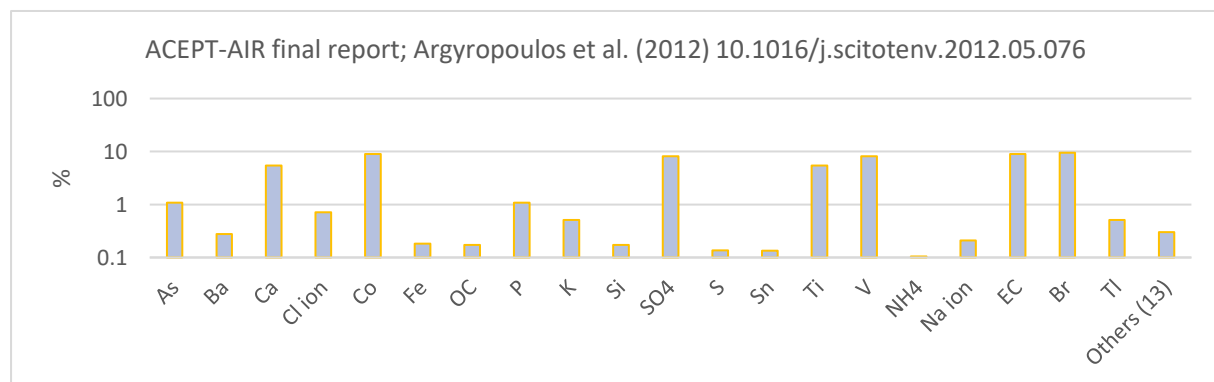


Figure 10. Open burning of crop residues chemical profile

Construction activities source profile is based on data obtained from Milan, Italy. Specific information's about sampling and analytical procedures used, were not provided. Calcium is most abundant element (19.85 %), closely followed by OC (17.9 %) and Si (12.55 %). Other metals including Ni (7.66 %), Al (3.78 %), Fe (1.91 %) and K (1.71 %) also have significant concentrations. Sulphates (9.14 %) and ammonium (1.96 %) are most abundant ions.

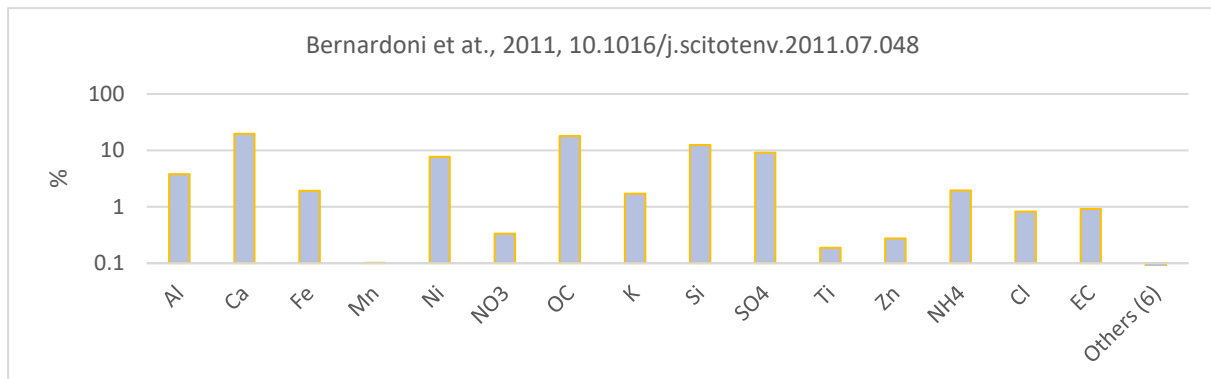


Figure 11. Construction activities chemical profile

Traffic source profile include two separate profiles, exhaust diesel and gasoline and urban traffic profile, based on data from PMF exercises in Valtellina, Po Valley, and Genoa Corso, Firenze in Italy. Specific information's about sampling and analytical procedures used, were not provided. OC and EC are most abundant compounds in both profiles, OC (53.59 and 35.1 %) and EC (30.46 and 23.04%) respectively. Some metals including Fe (13.56 and 2.34 %), Cu (1.1 %) and Si (0.89%) in mixed exhaust and Ca (1.89 %) in urban traffic mix, also have significant concentrations. Sulphates (5.05 %) are by far most abundant ion in mixed exhaust, while ammonium (1.68 %) and nitrates (1.51 %) are most abundant ions in urban traffic mix.

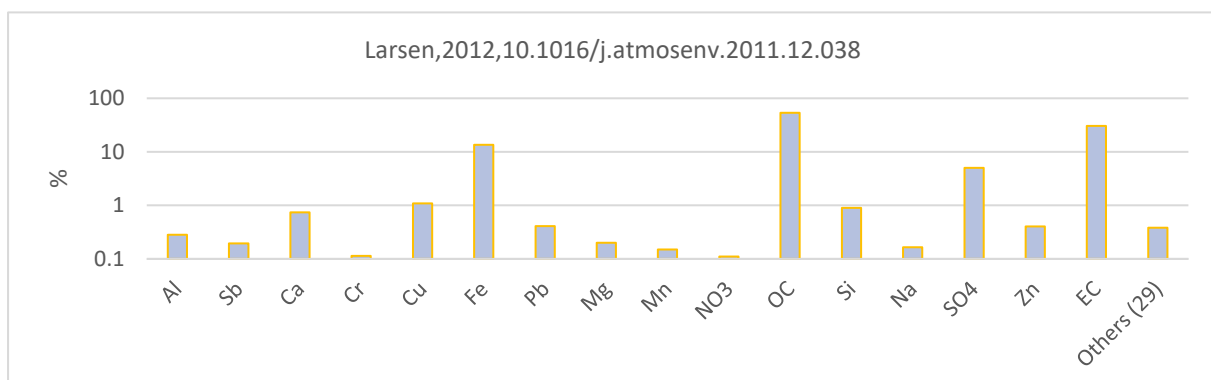


Figure 12. Exhaust diesel and gasoline chemical profile

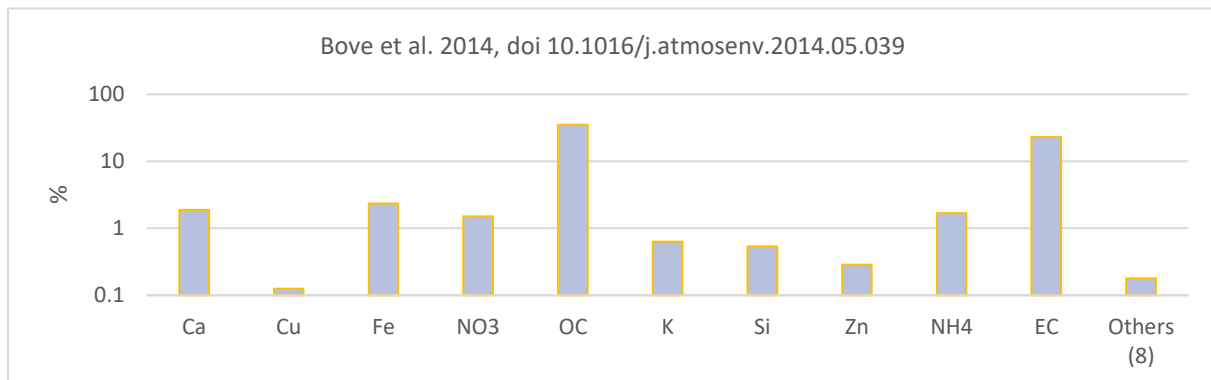


Figure 13. Urban traffic chemical profile

Road dust is another profile associated with traffic emissions. The profile selected is based on data from PMF exercises in Valtellina, Po Valley in Italy. Description of sampling and analytical procedures used, was not included. Silica is most abundant elements (15.63 %), followed from OC (7.25 %), Al (7.07 %), Fe (4.19 %), Ca (2.41 %), Mg (1.37%) and K (1.43 %). No significant concentrations of water-soluble ions were reported.

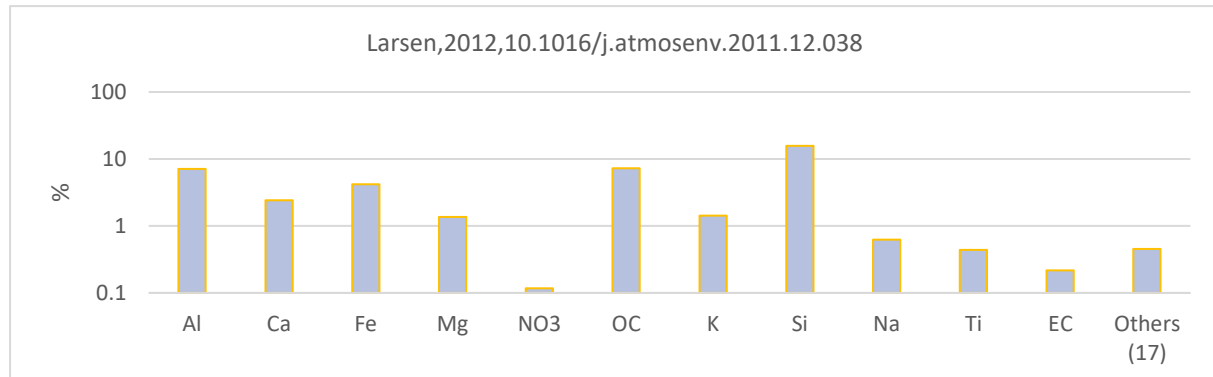


Figure 14. Road dust chemical profile

Soil dust profile is based on grab dust samples collected from the fabric filter from Thessaloniki area in Northern Greece. Samples were dried and resuspended in a puff of clean air, then sampled with PM10 inlet with LVS, and analysed using energy dispersive X-ray fluorescence (ED-XRF) for elemental composition and ion chromatography (IC) for water soluble ions analysis. Silica is most abundant element (20.9 %), followed by Al (5.65 %), Fe (4.36 %), Ca (3.20 %), Mg (1.56 %), K (1.37 %) and Ti (0.41 %). No significant concentrations of water-soluble ions were reported.

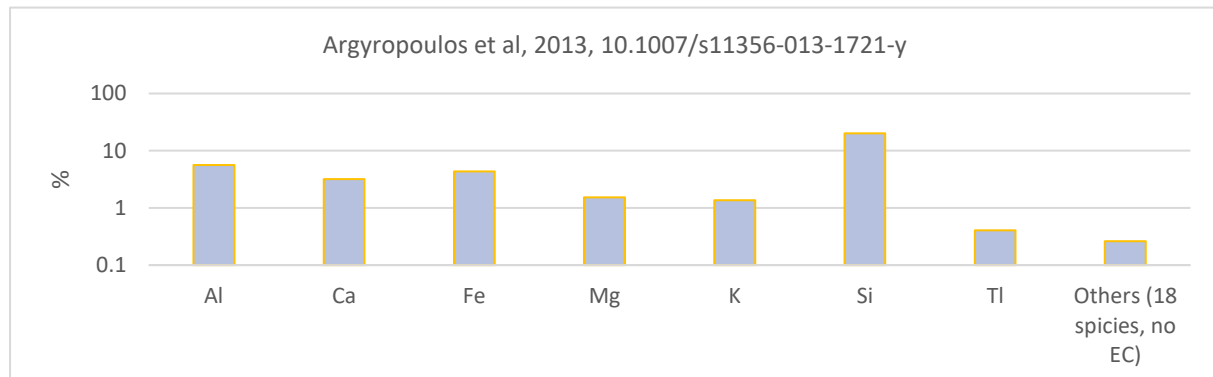


Figure 15. Soil dust chemical profile

Fuel and residual oils burning includes emissions from a wide range of sources, the majority of which are larger buildings heating systems (schools, hospitals, and other public institutions), industrial combustion emissions and to some extent older diesel-powered vehicles emissions.

Residual oil chemical profile is based on data from PMF exercise in Genoa Corso, Firenze in Italy. Samples were analysed using energy dispersive X-ray fluorescence (ED-XRF) for elemental composition, ion chromatography (IC) for water soluble ions analysis, and thermal optical analysis (TOT) for OC\EC analysis. Elemental carbon is by far most abundant compound (31.3%), followed by sulphates and ammonium ions (23 and 5.75 % respectively). As of metals, iron and vanadium exhibit highest concentrations (0.98 and 0.76 % respectively), followed by Ni (0.28 %), K (0.128 %) and Ca (0.10 %).

Fuel oil chemical profile is based on JRC data on small (<5MW) fuel oil boilers emission in Krakow, Poland. Specific information's about sampling and analytical procedures used, were not

provided. Organic carbon is most abundant compound (25.3 %), followed by nitrates (18.53 %) and sulphates (13.78 %). Other elements include Ca (1.2 %), Cl (1.16 %), Mg (0.57 %), Al (0.42 %), V (0.16 %) and Ni (0.14 %).

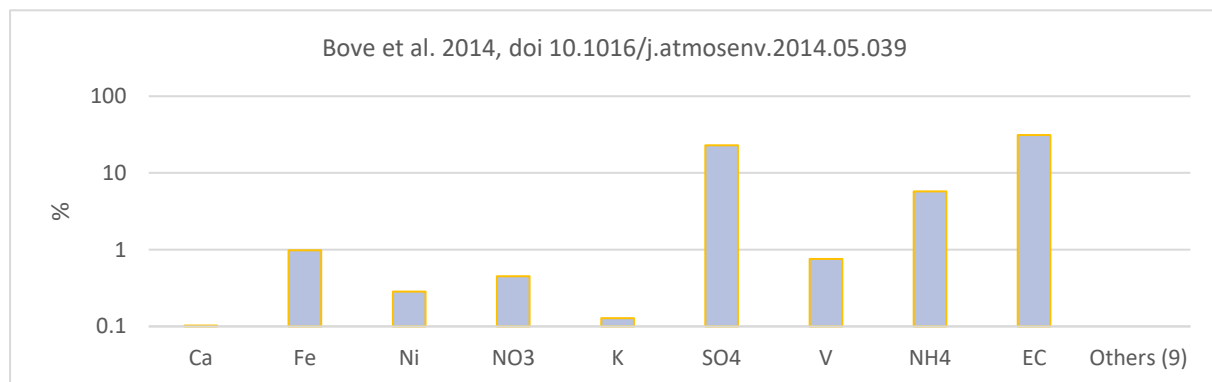


Figure 16. Residual oil chemical profile

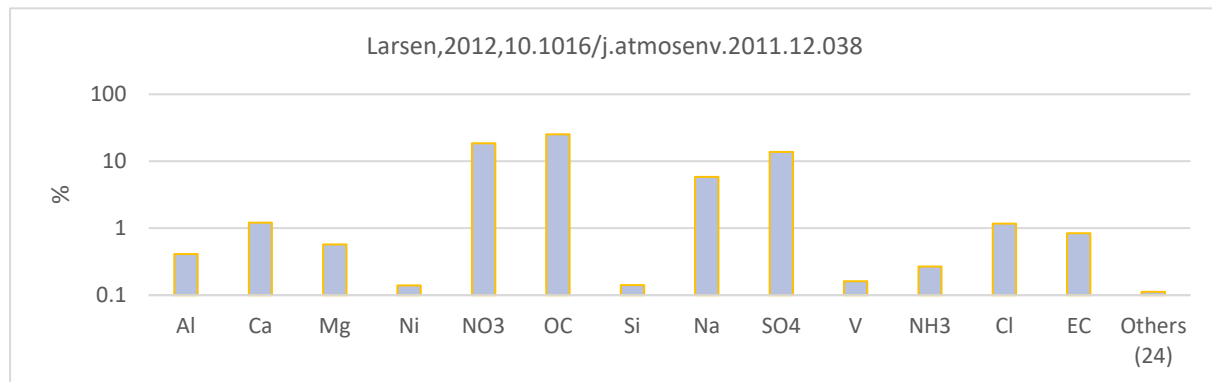


Figure 17. Fuel oil chemical profile

The source profiles outlined above were utilized to assign source categories to factors generated during positive matrix factorization. This procedure was supported with quantitative and descriptive comparison of the factor chemical profiles with those measured at the source and profiles from previous source apportionment studies in the literature, as given above.

4. Particulate matter sampling and analysis

Given the goals of the SA study, the available data, and the project document needs, we chose and set up one specific receptor/sampling point in the urban areas of Struga.

Due to the absence of a state network monitoring site in Struga, the laboratory AMBICON has installed a real-time particulate monitoring system certified as an indicative ambient monitor by M-CERT, and equipped with PC – data loggers and a WMO-grade data logging weather station (wind speed and wind direction). The network was operational as of March 2023.

The Struga sampling site, identified by our code MP4 - AQP - Struga, is situated within the premises of the "Niko Nestor" high school. The proximity to the closest road is around 5 meters. The first residential buildings, residences, and the school itself are located 20 meters away from the station. The distance to the city center is around 900 meters.



Figure 18. Monitoring location in Struga urban area

The sampling program at this location began on March 4, 2023. A 24-hour sample was collected bi-daily, culminating in a total of 180 samples by March 26, 2024.

All quality assurance and quality control protocols for the preparation, handling, and storage of the filters were executed in compliance with the Standard Operating Procedure of the UGD AMBICON Lab, which is accredited to ISO 17025 for environmental sampling and testing.

4.1. Sampling and determination of mass concentration of ambient particulate matter (PM2.5)

Sampling process was performed fully in line with the requirements of standard gravimetric measurement method for determination of the PM10/PM2,5 mass concentration of suspended particulate matter (EN 12341:2014). Sampling was performed on 47 mm PTFE filters (Advantec depth filter PF 020 and PF 040), according to Standard Operating Procedure of the UGD

AMBICON Lab, an ISO 17025 accredited for environment and samples from the environment testing (<https://iarm.gov.mk/en/2021/07/01/lt-052-university-goce-delcev-shtip/>).

Sampling procedure

The sampling site was equipped with low/medium volume sequential sampling system (PNS 18T-DM-6.1, Comde Derenda, Germany), certified as a reference device for PM2.5 sampling according to EN 12341:2014.

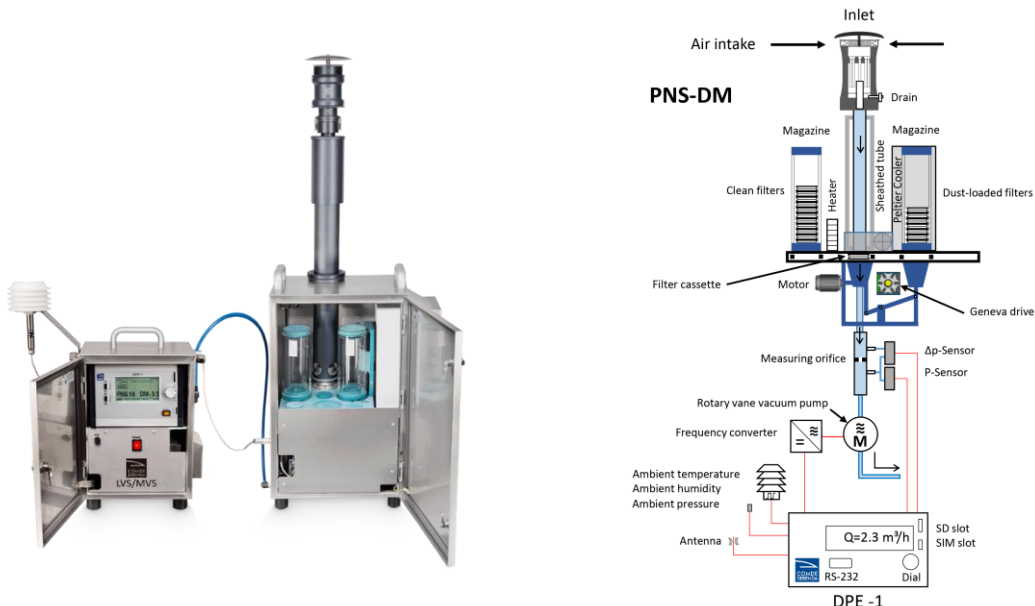


Figure 19. Sequential sampling system PNS 18T-DM 6.1

Sequential sampling systems provide fully automatic sampling according to pre-set parameters. Session from 14 to 16 days were set for each site. Each initial magazine was loaded in the AMBICON Lab premises with 16 to 18 filters, of which top one was not used for sampling, but as a protection in order to collect possible passive particle deposits. Additional one was transferred to the storage magazine without exposure and used as a field blank.

All monitoring data were electronically recorded, including sample ID, pump runtime, time of measurement, motor speed, actual flow, normalized flow, volume sampled-actual, volume sampled-normalized, filter pressure, ambient air pressure, outdoor temp, filter temp, chamber temp and relative humidity.

During each filter magazine change operation or at a period of 14 to 16 days, several quality assurance and control procedures were performed, including:

- sampling head cleaning,
- reading accuracy check for all sensors, and
- leak tightness test.

Sampling head, including inside of the tubular casing, the intake side of the multijet unit, the impaction plate and the jet tubes will be cleaned with alcohol and wiped with dry cloth. Impaction plate will be greased with silicone spray lubricant. The insect screen will be checked for obstructions and cleaned if necessary. Notes about cleaning and visual inspection were recorded in lab sampling logbook.

Reading accuracy of all sensors was checked through a short sampling test cycle, all the while, readings of the sensors was compared against external calibrated standards, including:

- test of flow rate set, against the reading of calibrated external flow meter (with certificate issued from ISO 17025 calibration lab),
- test of system temperature, humidity and ambient pressure readings, against calibrated external ambient Temp and RH meter (with certificate issued from ISO 17025 calibration lab),

Data about readings from all sensors were recorded in separate form of lab sampling logbook.

Leak tightness test of the system was performed through a low-pressure method, fully according to section 5.1.7.2 of the EN 12431:2014. The system has integrated leak test procedure, where pump is run, with closed calibration adapter until 400 hPa under-pressure in chamber is reached. The pump is switched off, and after 5 minutes pressure is read from the screen. If the value of under-pressure in the chamber is above 210 hPa, the system has passed the run test. According to above norm requirements, the test was repeated 3 times (total 3 runs). Data from the test runs were recorded in separate sheet of lab sampling logbook.

Filters handling and weighing

Prior to sampling, all filters were uniquely identified and conditioned at 19 °C to 21 °C and 45 to 50 % RH in climate chamber (ICH 110, Memmert, Germany) for ≥ 48 h, and weighted twice with at least 12 hours reconditioning period, to confirm mass stabilization (qualified difference < 40 μg). For each batch, two (2) blank filters are left to serve as a weighing room blanks.



Figure 20. Weighing room- AMBICON UGD Lab

After each sampling session, storage and initial magazine were removed from the housing. Protective reference filter was removed from the magazine and discarded, while empty magazine was fixed as new storage magazine. As soon as removed from the housing, storage magazine was sealed with cap and parafilm and stored in transportation “cool box”.

Sampled filters after exposure were returned to the weighing room and conditioned in a controlled temperature and humidity chamber for more than 48 hours and weighted. After additional conditioning period of minimum 24 hours, filters were re-weighted and accepted as stabilized if difference between results is $\leq 60 \mu\text{g}$. Same conditions was applied for filed blanks.

Weighing was performed with electronically controlled micro balance Radwag MYA5.3Y.F (resolution $d = 1 \mu\text{g}$), installed within controlled temperature and humidity room and completed with antistatic ionizer. Weighing data set and room conditions were electronically recorded.

Ongoing quality control were performed fully in line with the requirements of standard gravimetric measurement method for determination of the PM10/PM2,5 mass concentration of suspended particulate matter (EN 12341:2014), according to standard operating procedure of UGD AMBICON Lab, an ISO 17025 accredited for environment and samples from the environment testing areas.

Measurement uncertainties were calculated following GUM concept (JCGM 100) and included all individual uncertainty sources.

Mass concentration of ambient particulate matter was calculated as the difference in mass between the sampled and unsampled filter, divided by the sampled volume of air, determined as the flow rate multiplied by the sampling time. Measurement results are expressed as $\mu\text{g}/\text{m}^3$, where the volume of air is that at the ambient conditions near the inlet during sampling.

Data collected and comments are included in each filter testing results, given as supplementary material to this report (A – 1 Mass concentration of ambient particulate matter).

4.2. Chemical speciation

The elemental analysis of collected atmospheric aerosols (PM2.5) is the initial step in determining their sources and environmental impact. It can be accomplished by several methods. Certain analytical procedures are prohibitively expensive, others are labor-intensive, and some approaches result in sample destruction. This study utilized energy dispersive X-ray fluorescence (ED-XRF) for elemental composition analysis, optical transmissometer for measuring elemental carbon content, and spectrophotometry for the detection of water-soluble ions.

Elemental analysis using energy dispersive X-ray fluorescence spectrometry

The elemental analysis of PM2.5 of aerosols was conducted using energy dispersive X-ray fluorescence spectrometer NEX CG produced by Rigaku. The secondary targets of the NEX CG substantially improve detection limits for elements in highly scattering matrices including water, hydrocarbons, and biological materials, and a unique close-coupled Cartesian Geometry optical kernel significantly increases signal-to-noise. The spectrometer is capable of routine trace element analysis even in filter samples, thanks to the remarkable reduction in background noise and corresponding increase in element peaks [13].



Figure 21. NEX CG by Rigaku

Analyses were carried out in the AMBICON Lab, at Goce Delchev University in Shtip, North Macedonia, according to the EPA/625/R-96/010a Compendium of Methods, Method IO-3.3: determination of metals in ambient particulate matter using x-ray fluorescence (XRF) spectroscopy published by U.S. Environmental Protection Agency.

The calibration curve on the NEX CG was generated utilizing certified standard reference materials from UC Davis, Air Quality Research Center, University of California (USA), alongside SRM2783 from the National Institute of Standards and Technology (USA) and select single element certified reference materials from Micromatter (Canada). The calibration primarily utilized three multi-element reference materials, encompassing 28 components, which simulated atmospheric PM composition and covered a range from UC Davis. In addition to these three loaded filters, one UC Davis blank filter was also utilized.

Alongside continuous quality control and weekly monitoring of the certified reference filters (Table 2), we also ensure quality through inter-laboratory comparisons (Table 3).

Table 2. Quality control results of EDXRF NEX CG by Rigaku

Element	Certified reference concentration (ng/cm ²)	Average	Standard deviation	Coefficient of variation (%)	Recovery (%)
Na	178.43	149.76	31.18	20.82	100.0
Mg	89.84	89.11	3.88	4.36	100.0
Al	376.00	373.29	11.40	3.05	100.0
Si	1168.57	1159.05	21.19	1.83	100.0
P	9.17	9.09	0.27	2.95	100.0
S	1644.29	1644.29	46.11	2.80	100.0
K	2628.57	2640.00	25.50	0.97	100.0
Ca	3622.86	3623.81	22.91	0.63	100.0
V	8.20	8.17	1.13	13.81	100.0
Cr	81.00	82.80	2.12	2.56	100.0
Mn	24.99	26.66	3.00	11.27	100.0
Fe	733.14	728.86	14.74	2.02	100.0

Element	Certified reference concentration (ng/cm ²)	Average	Standard deviation	Coefficient of variation (%)	Recovery (%)
Co	37.43	41.63	5.24	12.59	100.0
Ni	60.00	64.76	5.03	7.76	100.0
Cu	26.50	28.15	5.70	20.23	100.0
Zn	103.30	105.21	5.57	5.30	100.0
As	142.17	151.95	25.94	17.07	100.0
Se	88.00	89.06	5.35	6.01	100.0
Zr	20.50	21.17	1.04	4.92	100.0
Mo	18.79	18.80	0.53	2.81	100.0
Cd	440.71	482.71	48.49	10.05	100.0
Ba	75.29	74.83	4.54	6.07	100.0
Pb	210.00	195.13	15.68	8.04	100.0

The inter-laboratory comparison was conducted directly between AMBICON Lab and the Institute of Nuclear & Radiological Sciences and Technology, Energy & Safety (INRASTES), affiliated with the National Center for Scientific Research Demokritos in Greece. A comprehensive comparison was performed using 21 PTFE filters with different loadings, comprising 20 samples and 1 blank.

The findings from the calculated Zeta-score have been considered acceptable, as presented in Table 3.

Table 3. Zeta-score results of EDXRF inter-laboratory comparison

Element	Zeta Score	Element	Zeta Score	Comments/Notes
Na	1.68	Ni	0.34	Explanation of Zeta-score values: $ z \leq 2.0$ the result is considered acceptable
Mg	1.21	Cu	2.31	$2.0 < z < 3.0$ indicate a warning signal
Al	1.69	Zn	0.80	$ z \geq 3.0$ results are considered unacceptable
Si	1.34	S	0,41	
Mn	1.04	K	0,67	
Fe	0.80	Ca	1.34	
Cr	0.39	Ba	2.49	
Pb	1.09			

Analysis of water-soluble ions

Water-soluble ions were extracted from the aerosol filters using sonication and shaking as recommended in the in-house developed Standard Operating Procedure for PM2.5 Cation Analysis [14]. The filters were cut in half using ceramic scissors and the mass of the filters was determined using electronically controlled micro balance with resolution of 1 µg. Half of the filter is placed in plastic centrifuge tubes filled with 25 mL ultra-pure water ($> 18\text{M}\Omega\text{-cm}$) and sonicated on room temperature in the ultrasonic bath (GT Sonic Pro, UK) for 60 minutes. Ice was added in the ultrasonic bath to keep the temperature below 27°C. After the sonication, the centrifuge tubes were shaken for 9 hours at 640 rpm using IKA KS 130 orbital shaker. After the procedure is completed, and in order to provide time for sample stabilization, the samples were stored in refrigerator overnight.

Water-soluble ions, including sulphates (SO_4^{2-}), nitrates (NO_3^-) and ammonium (NH_4^+) have been measured photometrically using the Spectroquant® Prove 600 spectrophotometer by Merck.



Figure 22. Spectroquant® Prove 600, Merck

Ammonium ions were analyzed using 1.14752.0001 Spectroquant® cell test analogous to EPA 350.1, ISO 7150-1 and DIN 38406-5 methods and detection limit of 0.015 mg/l NH₄⁺. Quality control was provided using Certipur - certified reference solution of NH₄Cl in H₂O (1000 mg/l NH₄⁺) traceable to NIST.

The sulphate ions were analyzed using 1.01812.0001 Spectroquant® cell test analogous to EPA 375.4, APHA 4500-SO₄²⁻E, and ASTM D516-16 methods and detection limit of 0.5 mg/l SO₄²⁻. Quality control was provided using Certipur - certified reference solution of Na₂SO₄ in H₂O (1000 mg/l SO₄) traceable to NIST.

Nitrate ions were analyzed using 1.09713.0001 Spectroquant® cell test analogous to DIN 38405-9in method and detection limit of 0.2 mg/l NO₃⁻. Quality control was provided using Certipur - certified reference solution of NaNO₃ in H₂O (1000 mg/l NO₃⁻) traceable to NIST.

Table 4. Quality control results for water soluble ions standard operating procedure

Ion	Concentration in certified reference solution		Average	Standard deviation	Coefficient of variation (%)	Recovery (%)
	mg/l	Certified reference solution				
NH ₄ ⁺	0,1	NH ₄ Cl in H ₂ O (1000 mg/l NH ₄ ⁺), Certipur	0,10	0,02	19,81	100,0
SO ₄ ²⁻	10	Na ₂ SO ₄ in H ₂ O (1000 mg/l SO ₄), Certipur	10,31	0,70	6,76	100,0
NO ₃ ⁻	10	NaNO ₃ in H ₂ O (1000 mg/l NO ₃ ⁻), Certipur	9,64	0,61	6,33	100,0

Elemental Carbon analysis

Black Carbon or Elemental Carbon was determined using Magee Scientific, SootScan™ Model OT21 Optical Transmissometer with dual wavelength light source (880nm providing the quantitative measurement of Elemental Carbon in PM, and a 370 nm for qualitative assessment of certain aromatic organic compounds), by applying EPA empirical EC relation for Teflon FRM filters.



Figure 23. Magee Scientific, SootScan™ Model OT21 Optical Transmissometer

The reproducibility of the photometric detector is validated using a Neutral Density Optical Kit, which is traceable to NIST and recommended by the manufacturer.

4.3. Observations and results

This sections present observations from the monitoring program conducted in Kumanovo, starting from March 2023 and ending March 2024. Results present daily variations in mass concentrations and chemical composition of PM with respect to various chemical species including carbon fraction (Elemental Carbon), crustal elements (Al, Si, Ca, Ti and Fe), water soluble ions (NH_4^+ , SO_4^{2-} , NO_3^-) and larger group of other elements (Na, Mg, P, S, Cl, K, V, Cr, Mn, Co, Ni, Cu, Zn, As, Se, Br, Rb, Sr, Zr, Mo, Cd, Ba, Pb).

Statistical Evaluation

Descriptive statistics help us summarize, describe, and illustrate the data in a more meaningful fashion, making data interpretation easier. Therefore, we provide a summary of descriptive coefficients for each of the sites included in the monitoring program below.

The descriptive statistical analysis presented includes both categories: measures of central tendency and measures of variability (or variation).

Measures of central tendency are techniques for describing the position of the centre of a frequency distribution for a given set of data. Although numerous statistics such as the mode, median, and mean can be used for this purpose, the middle position in this case is represented by the arithmetic mean.

Measures of variability provide a summary of a data set by illustrating the distribution of the observed results. Several statistics to explain this spread are utilized, including minimum, maximum, quartiles, variance, and standard deviation. Descriptive coefficients are combined with tabular and graphical descriptions, along with comments and discussions of the results.

Additionally, a correlation matrix illustrating the relationship between all values in the dataset is provided as a basic tool for summarizing large datasets and identifying and visualizing data relationships.

The correlation matrix table contains the correlation coefficients between each variable based on the Pearson parametric correlation test and is color-coded for correlation values above ± 0.6 . In this case, correlation matrices show how the species are related, pointing out their shared sources, and they are also used for exploratory factor analysis and checking data quality.

Table 5. Statistical evaluation – Struga dataset

	Units	N	Mean	SD	Minimum	Maximum	C.V.	95 th %	5 th %
PM2,5	µg/m ³	180.0	30.3	17.1	3.8	117.8	56.6	60.3	11.2
Na	ng/m ³	180.0	15.9	39.2	5.5	389.2	246.7	60.6	5.5
Mg		180.0	17.5	17.5	0.7	128.2	99.9	50.3	0.7
Al		180.0	109.8	107.5	0.5	870.5	97.9	307.2	8.1
Si		180.0	388.7	312.7	0.4	2396.6	80.4	971.7	55.5
P		180.0	1.9	1.3	0.0	9.9	71.0	4.3	0.2
S		180.0	117.5	87.0	0.2	399.3	74.1	278.9	7.9
Cl		180.0	27.9	64.0	0.2	615.7	229.5	108.4	0.2
K		180.0	150.0	130.6	1.0	771.0	87.0	419.6	37.2
Ca		180.0	1098.5	815.8	1.5	6355.3	74.3	2447.9	175.8
Ti		180.0	21.3	16.0	1.1	125.7	75.4	54.3	3.1
V		180.0	2.4	2.0	0.6	15.5	84.3	6.2	0.6
Cr		180.0	0.9	0.7	0.5	5.5	85.8	2.2	0.5
Mn		180.0	4.7	3.0	0.5	21.0	62.8	10.1	1.1
Fe		180.0	212.4	160.2	2.8	1259.8	75.4	516.4	29.8
Co		180.0	12.1	8.4	1.4	66.3	69.1	27.5	3.2
Ni		180.0	2.2	0.0	2.1	2.3	1.3	2.2	2.1
Cu		180.0	5.4	10.8	1.9	137.6	200.3	10.8	1.9
Zn		180.0	20.6	103.1	2.2	1391.2	499.4	31.9	2.2
As		180.0	0.7	0.9	0.2	10.2	123.7	1.2	0.2
Se		180.0	2.0	0.9	1.5	6.0	48.5	4.3	1.5
Br		180.0	2.0	2.5	0.7	29.7	127.9	3.3	0.7
Rb		180.0	1.5	0.9	0.6	4.8	56.6	3.0	0.6
Sr		180.0	9.1	6.1	0.2	21.3	66.7	17.6	2.1
Zr		180.0	3.5	2.4	0.0	18.0	66.8	7.5	0.4
Mo		180.0	1.3	1.0	0.0	4.6	73.8	3.2	0.1
Cd		180.0	0.6	0.5	0.0	2.7	83.5	1.6	0.2
Ba		180.0	25.2	19.1	1.3	149.1	75.7	65.1	3.3
Pb		180.0	8.6	17.1	3.7	229.7	198.6	15.3	3.7
EC		180.0	10190.0	5776.7	679.0	29949.0	56.7	18948.2	2179.5
NH ₄		180.0	399.7	342.3	9.1	1657.6	85.6	1091.0	45.3
SO ₄		180.0	3616.6	5952.9	9.1	44113.1	164.6	7400.2	464.7
NO ₃		180.0	331.4	633.0	9.1	2973.8	191.0	1920.3	9.1

Table 6. Correlation matrix – Struga dataset

	PM2,5	Na	Mg	Al	Si	P	S	Cl	K	Ca	Ti	V	Cr	Mn	Fe	Co	Ni	Cu	Zn	As	Se	Br	Rb	Sr	Zr	Mo	Cd	Ba	Pb	EC	NO	SO	NO3				
PM2,5	1.00																																				
Na	0.17	1.00																																			
Mg	0.31	0.46	1.00																																		
Al	0.29	0.40	0.99	1.00																																	
Si	0.35	0.41	0.98	0.99	1.00																																
P	0.36	0.33	0.78	0.74	0.78	1.00																															
S	0.35	0.13	0.51	0.47	0.47	0.58	1.00																														
Cl	0.13	0.88	0.21	0.12	0.15	0.18	0.04	1.00																													
K	0.43	0.48	0.56	0.51	0.56	0.45	0.33	0.52	1.00																												
Ca	0.46	0.38	0.58	0.54	0.66	0.62	0.29	0.30	0.58	1.00																											
Ti	0.33	0.39	0.96	0.97	0.98	0.75	0.46	0.14	0.54	0.62	1.00																										
V	0.32	0.39	0.95	0.96	0.96	0.74	0.49	0.14	0.53	0.60	0.97	1.00																									
Cr	0.25	0.33	0.81	0.83	0.82	0.58	0.37	0.06	0.43	0.44	0.81	0.80	1.00																								
Mn	0.39	0.39	0.93	0.93	0.95	0.76	0.49	0.16	0.56	0.65	0.94	0.93	0.80	1.00																							
Fe	0.36	0.37	0.95	0.97	0.98	0.77	0.46	0.10	0.50	0.63	0.98	0.96	0.83	0.97	1.00																						
Co	0.35	0.37	0.94	0.97	0.96	0.72	0.47	0.09	0.50	0.57	0.96	0.95	0.84	0.97	0.98	1.00																					
Ni	-0.13	0.15	-0.15	-0.17	-0.18	-0.20	-0.19	0.18	0.02	-0.14	-0.19	-0.18	-0.12	-0.18	-0.21	-0.17	1.00																				
Cu	0.20	0.10	0.15	0.13	0.14	0.18	0.29	0.07	0.05	0.15	0.11	0.16	0.14	0.15	0.15	0.15	0.15	0.12	1.00																		
Zn	0.03	0.73	0.08	0.03	0.03	0.08	0.02	0.71	0.13	0.04	0.03	0.04	0.06	0.07	0.03	0.04	0.25	0.12	1.00																		
As	0.11	0.67	0.19	0.15	0.15	0.18	0.17	0.62	0.20	0.07	0.14	0.16	0.17	0.20	0.15	0.17	0.17	0.24	0.83	1.00																	
Se	-0.12	0.20	-0.07	-0.06	-0.08	-0.10	-0.06	0.18	-0.07	-0.11	-0.07	-0.07	0.00	-0.06	0.01	0.13	0.02	0.32	0.29	1.00																	
Br	0.10	0.68	0.19	0.15	0.15	0.17	0.16	0.62	0.20	0.07	0.14	0.16	0.20	0.15	0.17	0.17	0.24	0.84	1.00	0.29	1.00																
Rb	0.08	0.31	0.22	0.23	0.19	0.06	0.19	0.25	0.27	-0.03	0.20	0.25	0.25	0.33	0.20	0.34	0.08	0.17	0.30	0.48	0.40	0.47	1.00														
Sr	0.02	0.04	0.21	0.23	0.17	-0.01	0.11	-0.07	0.05	-0.14	0.18	0.24	0.26	0.30	0.19	0.35	0.05	0.13	0.03	0.18	0.35	0.18	0.77	1.00													
Zr	0.36	0.29	0.73	0.68	0.72	0.99	0.66	0.16	0.42	0.56	0.69	0.53	0.71	0.71	0.67	-0.20	0.21	0.08	0.19	-0.09	0.18	0.09	0.02	1.00													
Mo	0.35	0.13	0.51	0.47	0.47	0.58	1.00	0.03	0.33	0.29	0.46	0.49	0.37	0.49	0.46	0.47	-0.19	0.29	0.01	0.17	-0.06	0.16	0.19	0.11	0.66	1.00											
Cd	0.43	0.48	0.58	0.54	0.58	0.44	0.34	0.50	0.99	0.57	0.56	0.55	0.45	0.60	0.53	0.54	0.02	0.06	0.14	0.22	-0.04	0.21	0.34	0.41	0.34	1.00											
Ba	0.33	0.39	0.96	0.97	0.98	0.75	0.47	0.14	0.54	0.62	1.00	0.97	0.81	0.94	0.98	0.96	-0.18	0.14	0.03	0.15	-0.06	0.15	0.20	0.19	0.69	0.46	0.56	1.00									
Pb	0.04	0.71	0.10	0.05	0.05	0.67	0.11	-0.01	0.05	0.06	0.09	0.10	0.05	0.08	0.23	0.21	0.97	0.85	0.36	0.85	0.41	0.16	0.08	0.05	0.13	0.05	1.00										
EC	0.29	-0.11	0.20	0.23	0.26	0.18	-0.19	-0.08	0.13	0.24	0.23	0.31	0.32	-0.33	0.11	-0.06	0.04	0.02	0.03	0.18	0.16	0.27	0.18	-0.06	0.01	0.23	0.01	1.00									
NH4	0.29	-0.13	0.07	0.05	0.04	0.24	0.78	-0.13	0.00	-0.06	0.05	0.12	0.07	0.10	-0.21	0.18	-0.05	0.07	-0.02	0.06	0.17	0.12	0.35	0.78	0.01	0.05	0.01	0.24	1.00								
SO4	0.49	-0.02	0.11	0.10	0.11	0.16	0.32	-0.04	0.12	0.05	0.10	0.11	0.09	0.15	0.11	0.13	-0.07	0.09	-0.02	0.03	0.15	0.08	0.20	0.32	0.13	0.10	0.02	0.13	0.37	1.00							
NO3	0.28	0.19	-0.01	0.00	0.04	-0.05	-0.08	0.34	0.62	0.27	0.06	0.04	0.03	0.11	0.05	0.04	0.05	-0.06	0.09	0.08	0.12	-0.09	-0.08	0.02	0.08	0.05	0.02	-0.10	-0.05	0.62	0.06	0.05	0.02	-0.10	-0.05	1.00	

Temporal variations

Temporal variations of PM2.5 concentrations help clarify the sources and contributing factors that lead to air pollution [15, 16]. Diurnal and seasonal trends can distinguish between traffic-related, industrial, and meteorological impacts on PM2.5 concentrations. A detailed understanding of PM2.5 temporal patterns can inform the development of effective strategies for managing air quality and policies [17]. This includes implementing targeted emission control measures, optimizing monitoring networks, and issuing timely public advisories. Since the temporal variations in PM2.5 are influenced by meteorological factors such as temperature, humidity, and wind patterns [18], comprehending these relationships is essential for assessing the potential impacts of climate change on air quality.

Temporal variations are assessed using gravimetric data in conjunction with real-time data from collocated referent monitoring stations. Modelling was conducted using the Openair R package, which is designed for analysing air quality data, or more broadly, atmospheric composition data. Academics, as well as the public and corporate sectors, widely use the package.

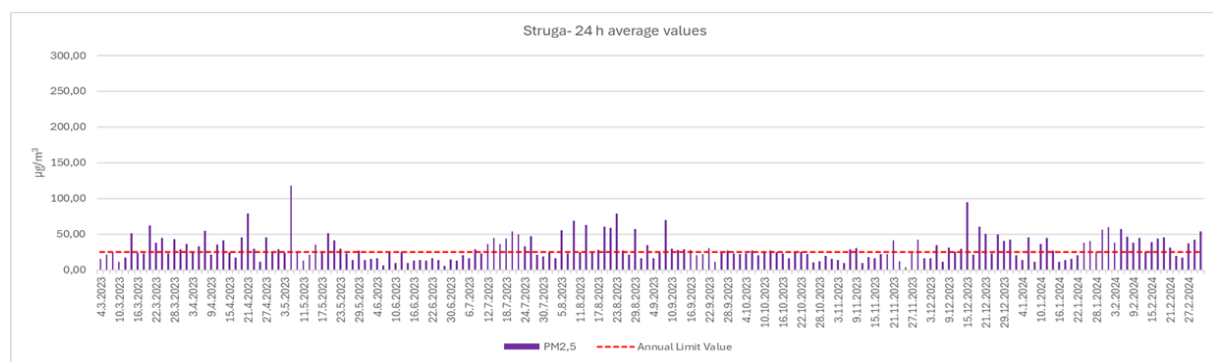


Figure 24. PM 2.5 – daily average concentrations from March 2023 to March 2024

The daily average PM2.5 concentrations measured at the Struga monitoring site exhibit significant daily and seasonal variations, exceeding all European Union limits, targets, and thresholds for human health protection. Daily readings exhibited considerable variability, with a Standard Deviation of $17.1 \mu\text{g}/\text{m}^3$ and a Coefficient of Variation of 56.6%. The concentrations ranged from a minimum of $3.8 \mu\text{g}/\text{m}^3$ to a maximum of $117.8 \mu\text{g}/\text{m}^3$, resulting in an average annual value of $30.3 \mu\text{g}/\text{m}^3$, which exceeds the annual threshold limit value of $25 \mu\text{g}/\text{m}^3$ by 21%. The percentage of days that exceeded the annual limit for PM 2.5 ($25 \mu\text{g}/\text{m}^3$) was notably high at 52.5% (94 out of 180 valid daily readings).

Surprisingly, there are no significant differences between the average concentrations during the warm and cold months. The average concentration during the heating season is $29.7 \mu\text{g}/\text{m}^3$, which is slightly (4%) lower than the average in the warm months. In the spring and summer months, the average value is $30.8 \mu\text{g}/\text{m}^3$, exceeding the annual limit value by approximately 23%.

Modelled data, however, show that there is no apparent variation in particulate matter concentration by day of the week or time of day during the spring, summer, or even autumn. On the opposite side, although there are no significant differences between the days of the week, during the winter there are expressed daily variations with distinct peaks in particulate matter levels at specific times of the day (early morning and especially late evening). This pattern is often influenced by an interaction of meteorological factors, anthropogenic activities, and local emissions, and is predominantly attributed to the increased utilization of woodstoves and other solid fuel heating means, which discharge substantial quantities of particulate matter into the atmosphere. The morning peak typically coincides with the initiation of daily activities, such as commuting and increased heating requirements, whereas the evening peak aligns with the return home and subsequent heating activities [19].

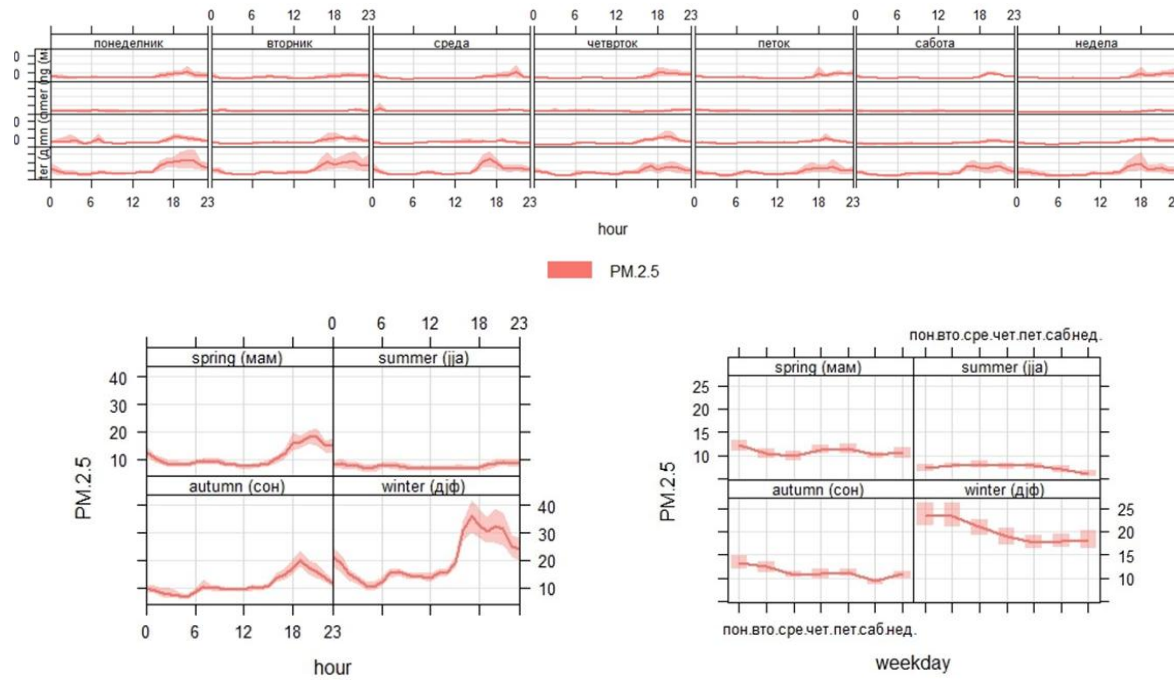


Figure 25. Daily variations in concentrations throughout all days, seasons, and weekdays

Correlation between meteorological conditions and PM concentrations

Bivariate polar plots are an effective analytical tool for understanding the origins and fluctuations of particulate matter, especially finer fractions like PM 2.5. These plots utilize polar coordinates to illustrate the correlation between wind speed and direction, enabling researchers to visualize the impact of these meteorological variables on PM concentrations. The radial axis (circles) commonly represents wind speed, whilst the angular axis signifies wind direction, aiding in the identification of major pollution sources according to their spatial distribution in relation to meteorological conditions.

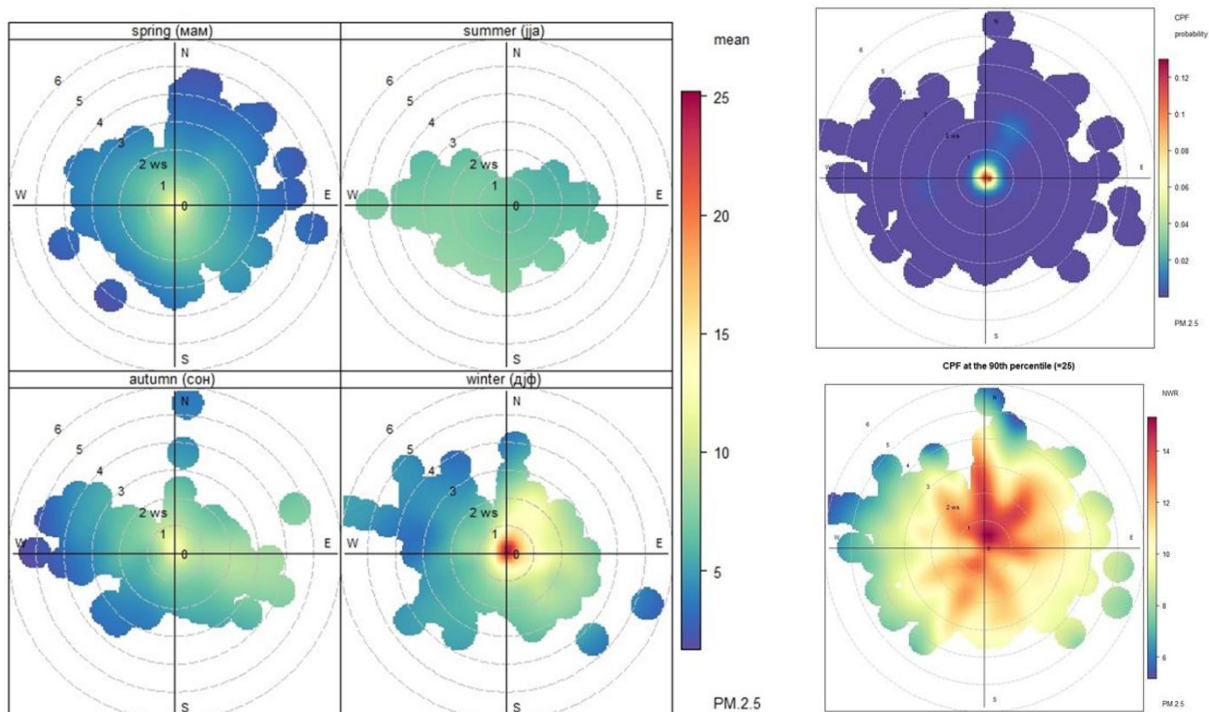


Figure 26. Bi-variate (seasonal), CPF and non parametric polar plots

Polar plots for the Struga area show that changes in concentration are mainly affected by local sources, as higher PM 2.5 levels are mostly seen during quiet winter weather, which usually has low wind speeds below 1 m/s. The conditional probability function supports this assertion by showing that higher particulate matter levels are mainly linked to low wind speeds, suggesting that these levels originate from local or nearby sources.

Additionally, non-parametric wind regression (NWR) plots were used as a different way to better understand where pollution comes from in relation to wind patterns. This method uses nonparametric kernel smoothers that give more importance to pollution levels based on how close they are to certain wind speeds and directions. The analysis indicates that most of the pollution is associated with weak winds blowing from the north and northeast, suggesting that the pollution is local, or from nearby settlements (Misleshevo, Moriosta, Draslajica and Vranishta) and the main roads. Given that this direction also corresponds with the urban area of the city, it implies that the sources of pollution are also within the city limits.

PM 2.5 chemical composition

The chemical compositions of PM2.5 differ across Europe and on average, Central Europe has more carbonaceous matter in PM2.5, North-western Europe has more nitrate, and southern Europe has more mineral dust in all fractions [20].

The contribution of mineral (soil) particles measured in Struga is similar like the values recorded in Skopje and is within the range identified in certain regions of Southern Europe, achieving an annual average of around 6% [20, 21]. Elements like Mg, Al, Si, Ca, Ti and Fe, usually used as tracers for soil dust, are well correlated, indicating common source for these elements and providing clear identification of this source in subsequent factor analysis.

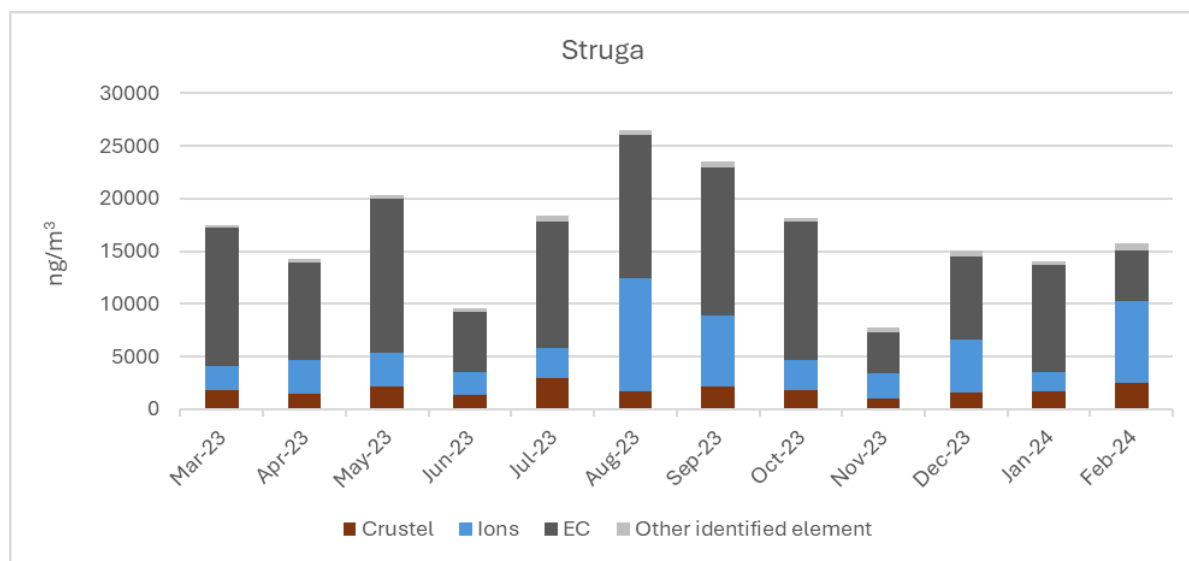


Figure 27. Major components and elemental groups identified

Sea salt contributions are negligible, as would be expected for a typically continental location. The contributions of ions (sulphates and nitrates) are markedly lower than those documented throughout Europe, with a combined contribution of 14% falling within the range of values observed in Skopje [20, 21]. This may be attributed to several factors; however, it is important to note the relatively low average concentrations of gaseous precursors such as sulfuric and nitrous oxides.

Elemental carbon (EC) contributions in the urban area of Struga exceed European averages, with an average of 34 %. This figure is also significantly higher than that observed in Skopje. This discrepancy likely reflects the local sources of emissions, with wood combustion identified as the most significant single source of particulate matter. Traffic emissions, particularly exhaust from service and older diesel-powered vehicles, can also impact this situation.

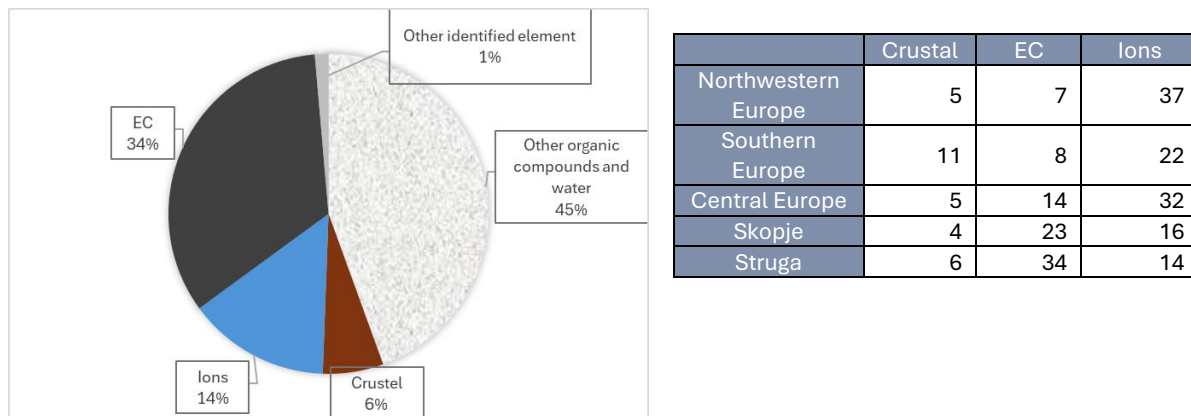


Figure 28. Contribution of major particulate matter components [20, 21]

Assessment of regulated metals, specifically lead, arsenic, cadmium, and nickel, was conducted only for those metals that successfully underwent external quality assessment procedures, encompassing only lead and nickel. The results for arsenic and cadmium are available; however, they are excluded from direct comparison due to significant uncertainty associated. It was determined that average annual concentrations of lead and nickel found were within the annual limit threshold values as specified in Directives 2008/51/EC and 2004/71/EC.

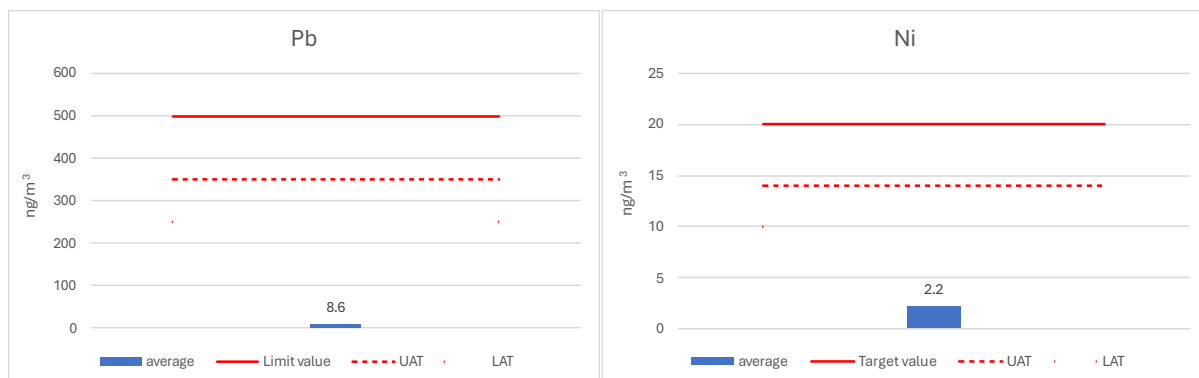


Figure 29. Average monthly concentrations of lead (Pb) and nickel (Ni) in Struga

5. Positive Matrix Factorisation

Environmental monitoring data are increasingly being handled in terms of mathematical models, which allow for the management of a variety of datasets with multiple observations to be performed. Different modeling techniques are available depending on the type of known information (input data) and the sort of results that would be obtained (output data) that are desired.

Source apportionment (SA) is the practice of obtaining information about pollution sources and the amount of pollution that each source contributes to the level of ambient air pollution. Emission inventories, source-oriented models, and receptor-oriented models are three methods that can be employed to accomplish this task.

In recent years, receptor-oriented models (also known as receptor models (RMs)) have gained prominence in environmental sciences. These models are utilized to extract information from datasets containing various features (chemical or physical properties) associated with the measured samples. For instance, they can assess the contribution of contamination and pollutant sources across different sample types, beginning with the data provided by the samples (recorded at the monitoring site) and advancing to the point of effect, or receptor.

Receptor models are also referred to as multivariate methods because they analyze datasets that consist of numerous numerical values as a whole. More specifically, receptor models are mathematical methodologies designed to quantify the contribution of sources to samples based on their composition or fingerprints. To differentiate impacts, the composition or speciation is identified using media-specific analytical methods, and the identification of key species or combinations of species is necessary. A speciated data set can be considered of as a data matrix X with i by j dimensions, in which i samples and j chemical species were measured with u uncertainty.

The goal of receptor models is to solve the chemical mass balance (CMB) in Equation 1, between measured species concentrations and source profiles, where p is the number of factors, f is each source's element profile, g is each factor's mass in each sample, and e_{ij} is the "remaining" for each element/sample.

$$x_{ij} = \sum_{k=1}^p g_{ik} f_{kj} + e_{ij} \quad (1)$$

A dataset containing a vast amount of data consisting of chemical elements (such as elemental concentrations) acquired from a large number of observations (samples) is required to find the answer. The larger the data matrix, the more likely the model is to uncover separate factors that can be used as sources. The number of samples required can vary depending on prior knowledge of the sources and the RMs methodology chosen (e.g., CMB vs. PMF).

If the number and nature (composition profiles/fingerprints) of the sources in the study area are known, then the only unknown term of equation (1) is the mass contribution of each source to each sample. To solve the chemical mass balance and to elicit information on sources type, number and contribution starting from observations (i.e. element concentrations data set) at receptor site, different factor analysis methods (multivariate methods) have been developed. Common factor analysis methods used include Principal Component Analysis (PCA), Unmix, Target Transformation Factor Analysis (TTFA), Positive Matrix Factorization (PMF) and Multilinear Engine (ME).

Dr. Pentti Paatero (Department of Physics, University of Helsinki) created Positive Matrix Factorization (PMF) in the mid-1990s to establish a new method for the analysis of multivariate data that addressed several drawbacks of the PCA.

PMF uses error estimates to weight data values and imposes non-negativity constraints in the factor computational process. The algorithm accomplishes weighted least squares fit with the objective of minimizing Q, a function of the residuals weighted by the uncertainties of the species concentrations in the data matrix. The PMF factor model can be written as $X = G \cdot F + E$, where X is the known $n \cdot m$ matrix of the m measured chemical species in n samples. G is an $n \cdot p$ matrix of factor (source) contribution in every sample (time series). F is a $p \cdot m$ matrix of factor compositions (factor profiles). G and F are factor matrices to be determined and E is defined as a residual matrix, i.e. the difference between the measured X and the modeled Y = G·F.

In this study, the free software US-EPA PMF 5.0 version 5.0.14 [22], implementing the ME-2 algorithm developed by Paatero (1999), was used.

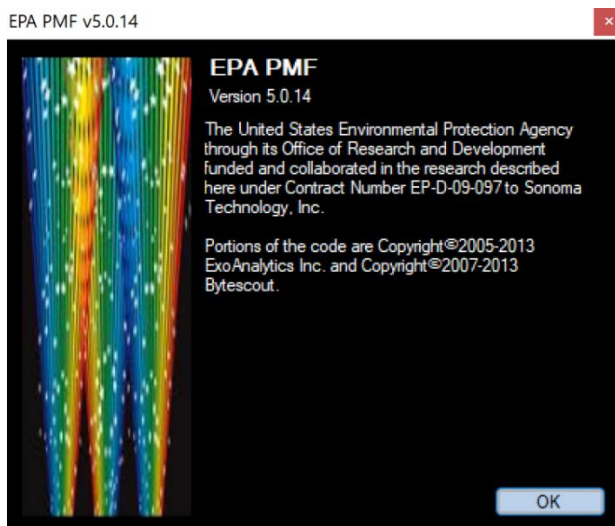


Figure 30. Free software US-EPA PMF 5.0 version 5.0.14 – splash screen

PMF was first employed in studies of air pollution and source apportionment [23, 24] as well as precipitation investigations [25]. Air quality and source apportionment applications [26, 27] have gained rapid popularity in recent years, but PMF has also been used on lake sediments [28], wastewater [29, 30], and soils [31]. This multivariate factor analysis tool has been used to analyze a variety of data, including 24-hour speciated PM2.5, size-resolved aerosol, deposition, air toxics, high time resolution measurements from aerosol mass spectrometers (AMS), and volatile organic compound (VOC) data.

The use of known experimental uncertainties as input data allows for individual handling of matrix members and can handle missing or below-detection-limit data, which is a prevalent feature of environmental monitoring. Because the PMF results are quantitative, it is feasible to determine the composition of the sources determined by the model.

Equation 2 was used to determine the uncertainty of the utilized method for each element separately, and Equation 3 was used to determine the uncertainty of the instrument for each element separately:

$$u = \sqrt{U_{instrument}^2 + U_{CRM}^2 + U_{sampling}^2} \quad (\%) \quad (2)$$

$$U_{instrument} = \frac{STDEV}{average} * 100 \quad (\%) \quad (3)$$

Where $U_{instrument}$ - uncertainty of the used instrument, U_{CRM} - uncertainty of the used certified referent material, $U_{sampling}$ - uncertainty of the sampling.

Before data processing, various basic statistical tests—such as dispersion, distribution, correlation matrices, linear regression, and time trends—were conducted to examine the relationships among the variables.

5.1. Input data and PMF model setting

Species lists included water-soluble ions NH_4^+ , SO_4^{2-} , NO_3^- , elemental carbon (EC), and following elements; Na, Mg Al, Si, Ca, K, Ti, Fe, P, S, Cl, V, Cr, Mn, Co, Ni, Cu, Zn, As, Se, Br, Rb, Sr, Zr, Mo, Cd, Ba and Pb.

Following the EU protocol for receptor models [32], the data were initially processed to remove values that could potentially degrade the quality of the analysis. To validate the data and identify atypical values when compared to the rest of the dataset, scatter plots and time series analysis were employed. After data validation, the original datasets included 32 species and 180 daily samples.

As recommended in EU protocol for receptor models [32], data below the limit of detection (LOD) were substituted by half of the LOD and the uncertainties were set to 5/6 of the LOD. Missing data were substituted by the geometric mean of the measured concentrations and the corresponding uncertainties were set as 4 times this geometric mean [33].

Species with high noise were down-weighted based on their signal-to-noise (S/N) ratio to reduce the influence of poor variables on the PMF analysis. Species with S/N lower than 0.5 were considered as bad variables and excluded from the analysis, and species with S/N between 0.5 and 1 were defined as weak variables and down-weighted by increasing the uncertainty as recommended in the PMF users guideline. Using this approach Ni, As and Cd were set as a weak variables. The EC also was set as a weak although S/N was above 8. PM 2.5 was also set as total (week) variable in order to reduce influence on profiles contribution.

Additional information regarding the modelling approach is provided in Source Apportionment Study for Skopje urban area –identification of main sources of ambient air pollution [34]

5.2. Factor attribution to sources

Final PMF solution for Struga datasets included 6 factors. Factors were attributed to their sources through a quantitative and qualitative comparisons of the factor chemical profile with PM profiles reported EC-JRC SPECIEUROPE data base and profiles from previous source apportionment studies available in the literature. In addition, the standardised identity distance (SID) and the Pearson coefficient, expressed as Pearson distance ($\text{PD} = 1 - r$), were used to calculate the similarity between the factors and the reference source profiles available in the public datasets: EC-JRC SPECIEUROPE and US-EPA SPECIATE [35]. The Delta SA tool [10] was used to complete the work.

Factors that were identified in municipality of Struga are as follows: biomass burning, traffic, fuel and residual oil, road and soil dust, open fire and waste burning and secondary aerosols.

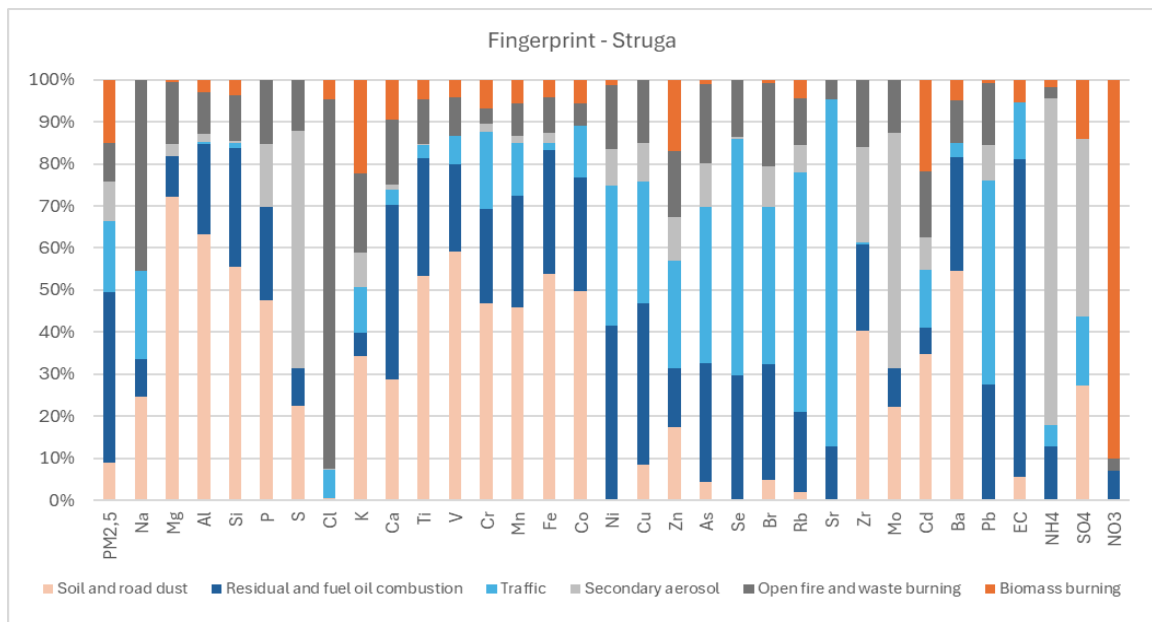


Figure 31. Factor fingerprint for Struga

Biomass burning incorporates emissions from different types of woodburning stoves and boilers used mostly in residential heating. Key species found in this factor include EC, K, Cl, NO_3^- and Rb. K is produced from the combustion of wood lignin [36, 37]. Although this element can be emitted from other sources, such as soil dust [38], K has been used extensively as an inorganic tracer to apportion biomass burning contributions to ambient aerosol and was associated with biomass burning in PMF source profiles in Tirana, Skopje, Athens, Belgrade, Banja Luka, Debrecen, Chisnay, Zagreb and Krakow [39].

Cl can be emitted from biomass burning and also from coal combustion, especially during the cold period [40]. It is also associated with biomass burning in PMF source profiles in Belgrade and Banja Luka [39]. In addition, NO_3^- , and NH_4^+ also contributed significantly to the biomass burning factor. Biomass burning is an important source of NH_3 [41] which rapidly reacts with HNO_3 to form NH_4NO_3 aerosols. The presence of NH_4NO_3 aerosols in biomass burning plumes, has also been reported previously [41, 42].

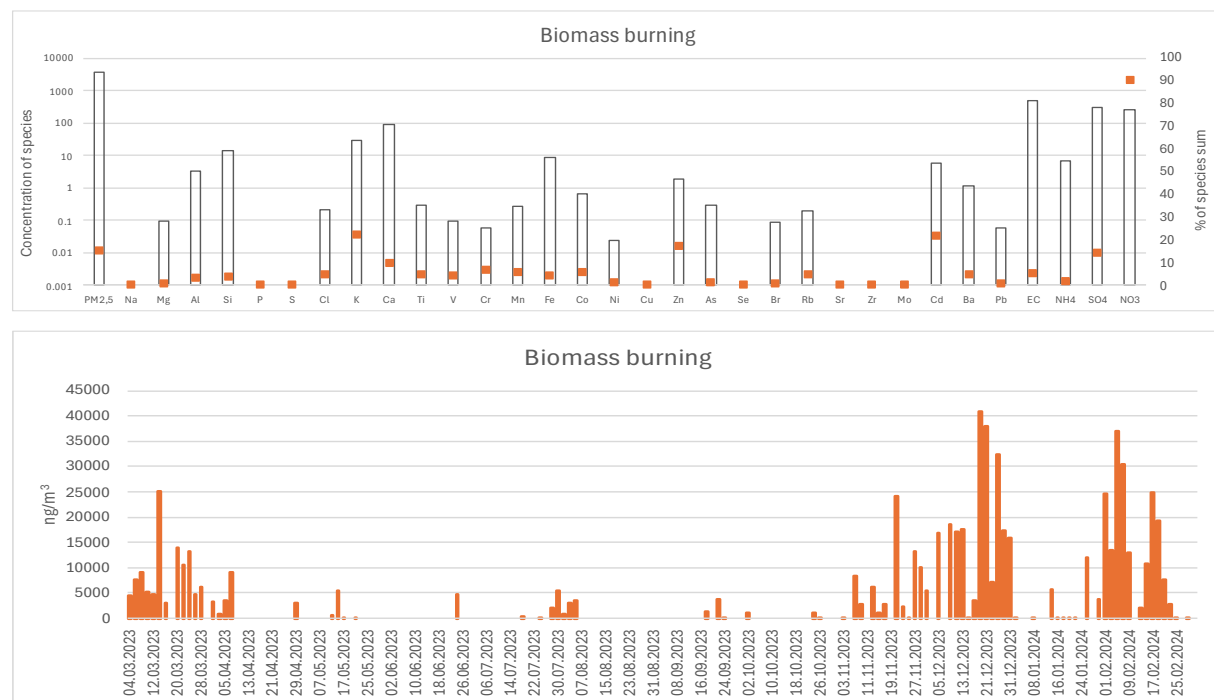


Figure 32. Biomass burning factor profiles in Struga

Evaluation of seasonal pattern of this factor clearly confirm attribution of this factors to biomass burning emissions that usually occur only during the cold months.

Traffic includes particles from several different sources including vehicles exhaust, mechanical abrasions of brakes and tires, road (resuspended) dust and road salting. All sources associated have their own specific fingerprints, and can be identified by EC, Ba, Cu, Mn, Pb and Zn, as well as crustal species like Mg, Al, Si, Ca, Fe, and Ti, or Na and Cl in the case of winter road salting.

The vehicle exhaust, including diesel and gasoline, consist high percentage of organic and elemental carbon, Fe, Pb, Zn, Al, Cu and sulphate. Similar species were also associated with traffic in PMF source profiles in most European and Central Asia urban areas [39].

Zn is a major additive to lubricant oil. Zn and Fe can also originate from tire abrasion, brake linings, lubricants and corrosion of vehicular parts and tailpipe emission [43-46]. As the use of Pb additives in gasoline has been banned, the observed Pb emissions may be associated with wear (tyre/brake) rather than fuel combustion [47].

Fe and Al is likely associated with vehicles part wear, such as tyre/brake wear and road abrasion, and are common species in case sampling sites are located close to major roads.

These results indicate the contribution of both exhaust and non-exhaust traffic emissions to various factors associated with traffic. The elemental composition of particulate emissions linked to traffic can vary significantly due to differences in traffic volume and patterns, vehicle fleet characteristics, climate, and the geology of the region [48]; however, similar elements (Cu, Mn, Zn, Pb, Fe, and EC) have been identified as key species in PMF source profiles across most urban areas in Europe and Central Asia [39].

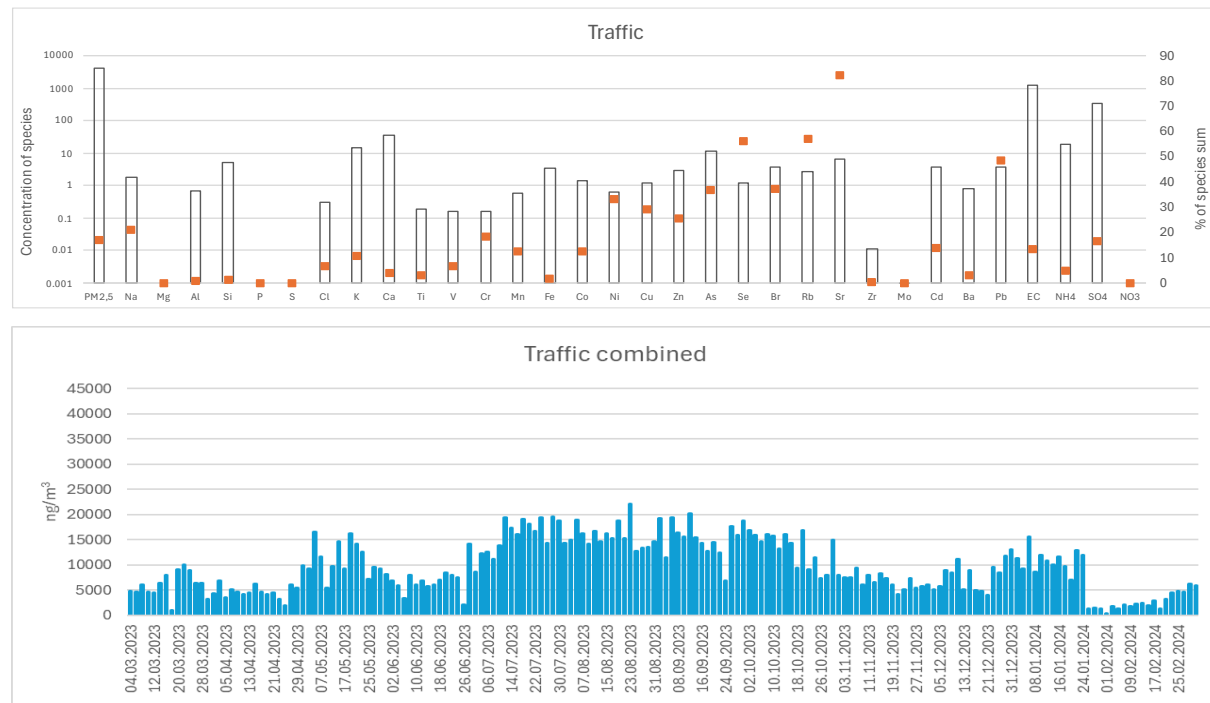


Figure 33. Traffic associated factors for Struga dataset

Fuel and residual oil combustion is a stand-alone factor that includes emissions from a wide range of sources, the majority of which are larger buildings heating systems (schools, hospitals, and other public institutions), industrial combustion emissions and to some extent older diesel-powered vehicles emissions, principally composed of EC, V, Cd and Ni [41, 42].

Organic carbon, sodium, and water-soluble ions including nitrates and sulphates are common key species for fuel oil emissions. The presence of V and Ni is also common marker. Water-

soluble ions, V, Fe, and Ni are also important species for residual oil combustion, but increased quantities of elemental carbon, rather than organic carbon, are common for this source.

Vanadium, either alone or in conjunction with nickel, is a prevalent marker in PMF source profiles, in most European and Central Asian urban areas [39].

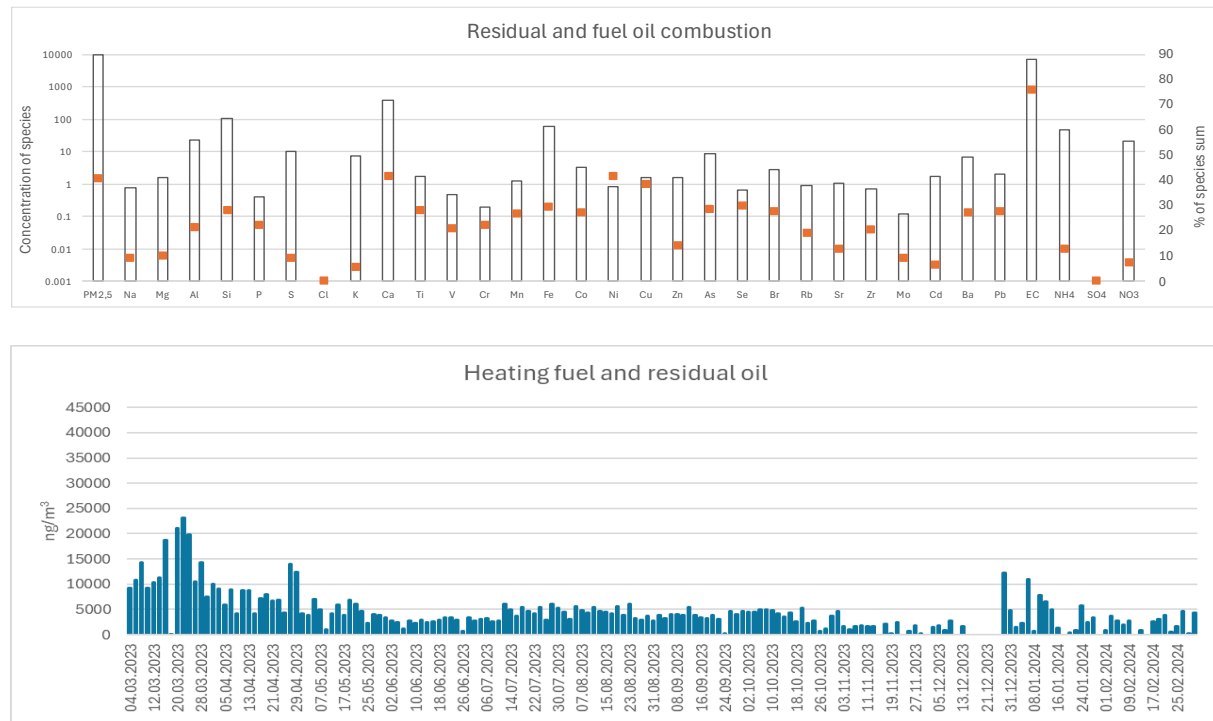


Figure 34. Fuel and residual oil factor profiles

Soil or mineral dust usually originates from construction/demolition activities, dust resuspension and wind erosion processes. This source is commonly identified with so called crustal elements like Mg, Al, Si, Ca, Fe and Ti [49]. Silicon and Ca are usually most abundant elements, followed by Fe, Al, Mg, and Ti with variations due to local geology.

Other research studies also reported significant contribution of soil dust to PM2.5 mass, suggesting that soil dust is an important contributor to PM2.5 mass especially in summertime [50, 51]. Similar elements (Ca, Fe, Al, Si, Ba, Na and Ti) were identified as key species in PMF source profiles in most European and Central Asia urban areas [39].

Silicon and calcium are also prevalent species in the construction related source's chemical profile. Chemical profile of construction source also includes Si, Ca, Al and Fe, but also OC, EC and sulphates have significant contribution.

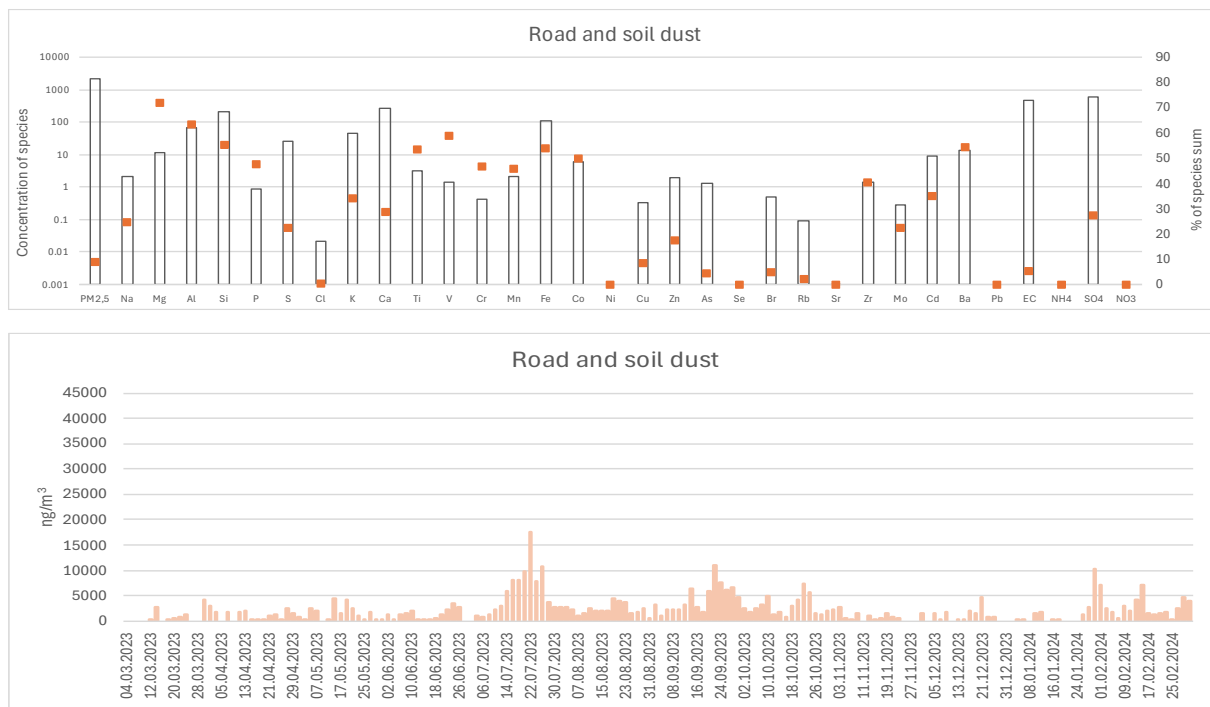


Figure 35. Mineral dust factor profiles

All types of low efficiency burning of agricultural and garden waste, as well as other types of waste, are classified as open fire burning. This factor is identified by high contribution Cl, As, Cd and Rb, but also includes some specific metals like Pb, Cu and Ni. Elemental carbon, Br, Co, V, Ti, and As were also found as important species in an analysis of agricultural waste open burning profiles, conducted in the Thessaloniki area in Northern Greece (SPECIEUROPE data base). According to Lemieux [52] depending on the source, varying amounts of metals such as lead (Pb) or mercury (Hg) may be emitted. Polychlorinated dibenzo-p-dioxins and polychlorinated dibenzofurans (PCDDs/Fs) or polychlorinated biphenyls (PCBs) can be emitted as well.

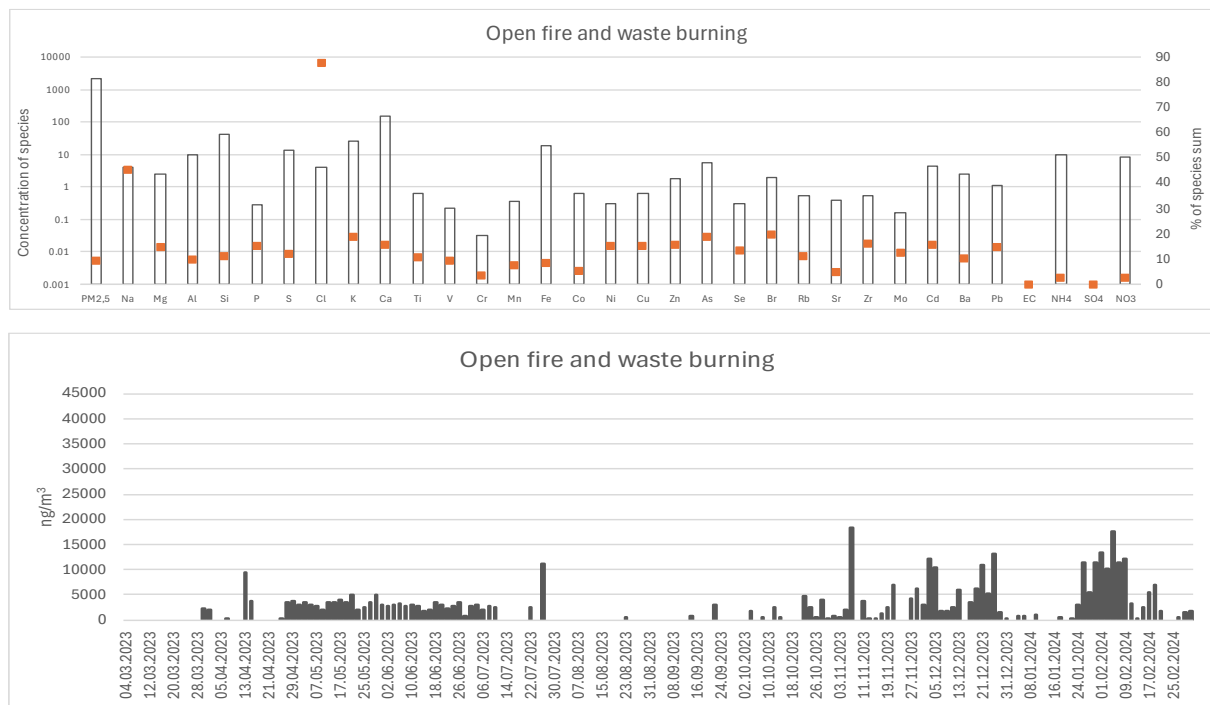


Figure 36. Open fire burning factor profile

Secondary aerosols contribute the most during the coldest and warmest months, when there are high levels of gaseous precursors in the winter and high temperatures in the summer.

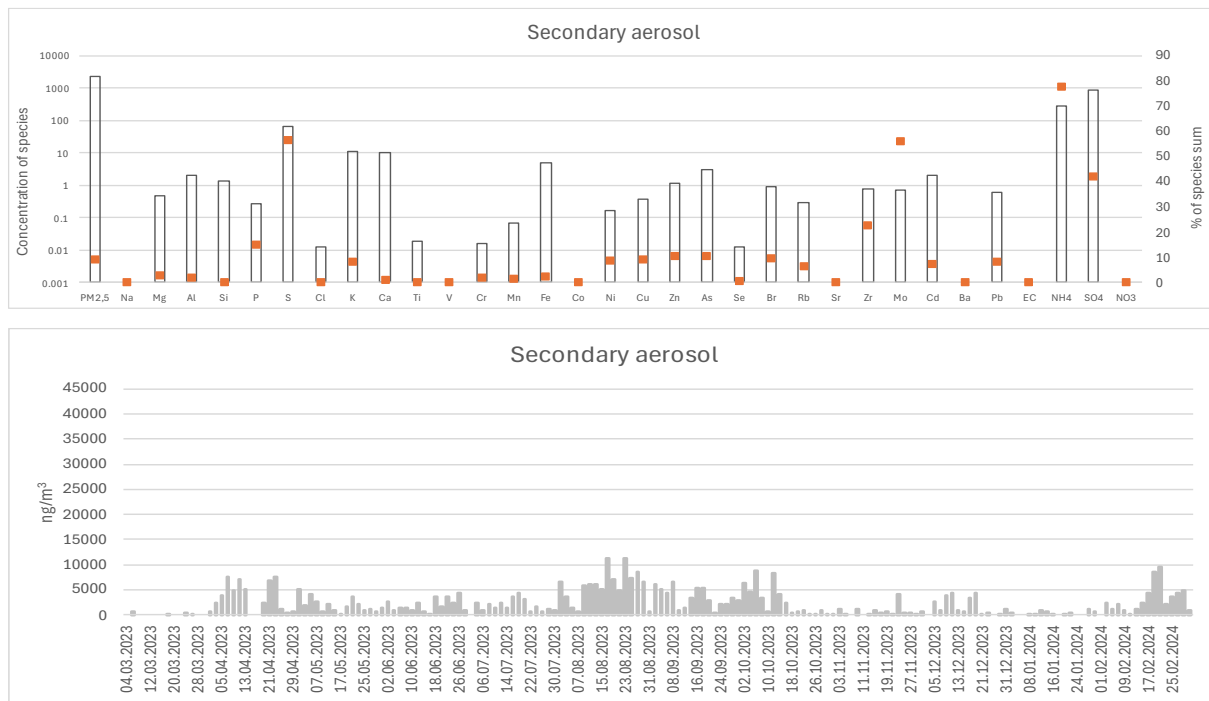


Figure 37. Secondary Aerosols factor profile

5.3. Sources Contribution

The contribution of each source to the total particle mass (PM 2.5) was determined using data from measurements and modelling exercises. The primary sources identified for Struga include biomass burning, open fires and waste burning, traffic, secondary aerosols, road and soil dust, and fuel and residual oil combustion. The traffic contribution was determined by combining modelled values from two identified sources: traffic and the combustion of fuel and residual oil. Because of the resemblance in exhaust emissions from older diesel vehicles and fuel oil-burning boilers, a significant amount, 70 %, of fuel oil contributions during warmer periods are attributed to traffic sources.

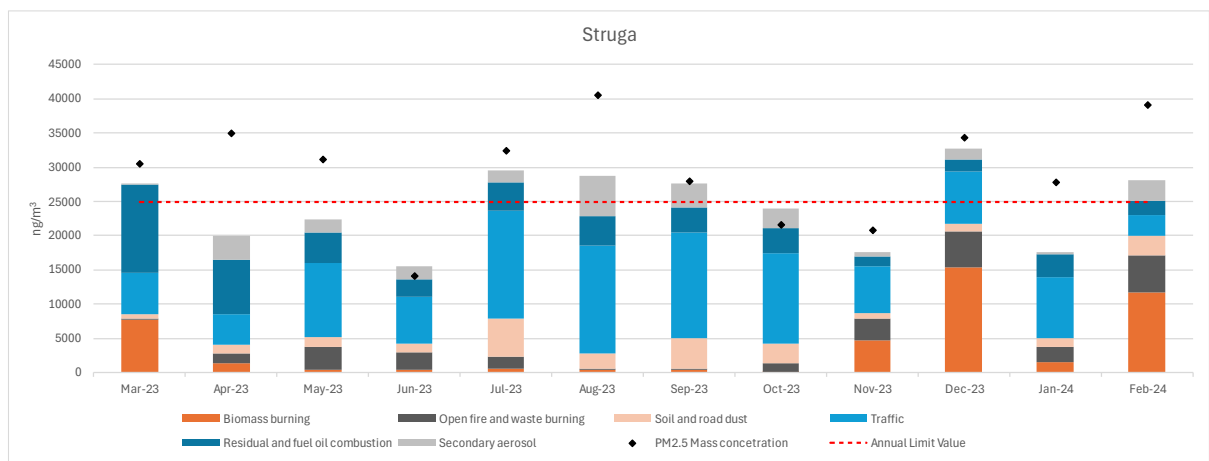


Figure 38. Average monthly contributions to total particulate mass (PM 2.5) – Struga

The traffic represents the primary air pollution source, demonstrating a steady contribution throughout the year, with a notable increase during the summer and fall months, ranging from 2.9 to 15.7 $\mu\text{g}/\text{m}^3$. The annual relative contribution of traffic constituted 40 % of the total particulate mass (PM 2.5), with monthly relative contributions up to 55.7 %. This source includes

emissions resulting from vehicles exhaust, brake and tire wear, in addition to the combustion of oil in older diesel engines, such as those found in tractors, trucks, and older passenger vehicles lacking exhaust control devices.

Combustion of fuel and residual oil mainly comes from furnaces for heating public facilities and buildings (kindergartens, schools, hospitals), as well as in industrial facilities for heat production or some other technological processes. Fuel and residual oil contribute from 1.4 and 7.9 $\mu\text{g}/\text{m}^3$ to total particulate mass. This source occurs consistent over the year. Annual relative contribution of fuel and residual oil combustion accounted for 18 % of the total particulate mass (PM 2.5) mass. Relative monthly contribution ranged from 5.2 to 40 %.

Biomass burning was also significant source in the municipality of Struga during the winter months, with the biggest contribution to total particle mass occurring in November, December, January, February, and March, while having minimal impact during the summer months. Biomass burning mostly belongs to residential heating; however, it also includes biomass burning in bakeries, restaurants, and small industrial establishments that utilize wood for heating or generating thermal energy for their operational processes. The average monthly contribution of biomass burning over the winter season is up to 15.4 $\mu\text{g}/\text{m}^3$. The relative contributions (%) of biomass burning to total particle mass demonstrate significant seasonal variability, with this source accounting up to 50 % during winter months, and although entirely seasonal, biomass burning accounts for a significant annual relative contribution of 15 %.

Road and soil dust, additionally referred to as mineral dust, comprises particulate matter primarily originating from construction activities and the resuspension of deposits on roadways. This source significantly contributes to total particulate mass (PM2.5), with an increasing contribution during dry seasons. Mineral dust contributes from 0.6 to 5.5 $\mu\text{g}/\text{m}^3$ to total particulate mass. The monthly contributions from this source vary between 2.4 % and a significant 18.6 %, but the annual relative contribution attains a notable 9 %.

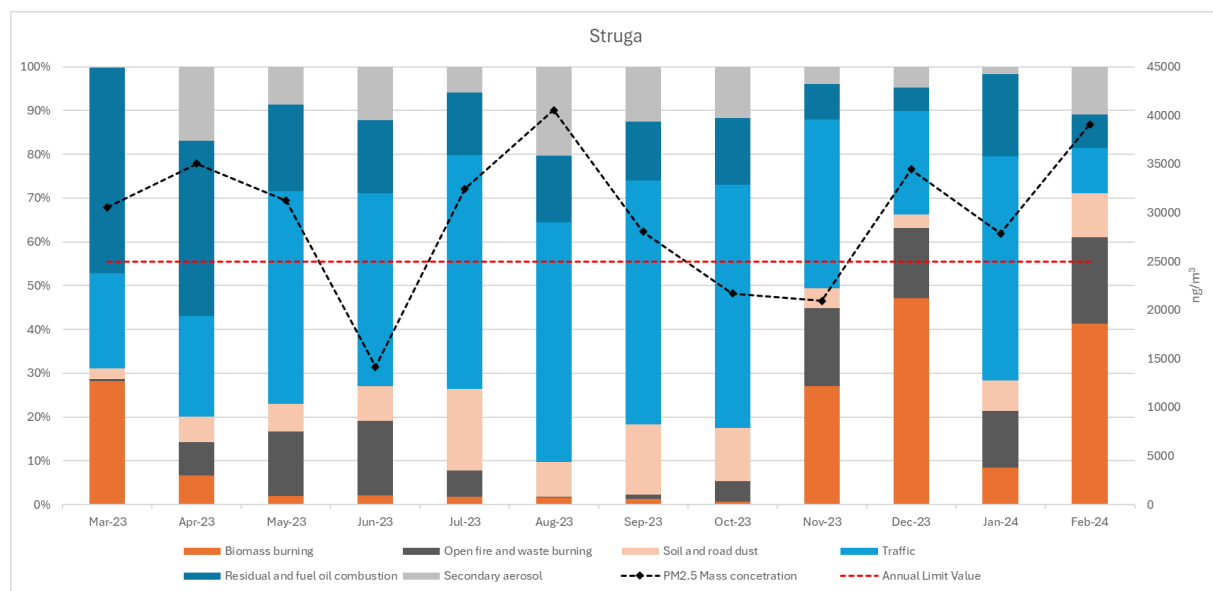


Figure 39. Relative monthly contribution – Struga

Open fires and waste burning include the combustion of crop residue, agricultural and garden waste materials, as well as landfill fires and wildfires. This factor also includes the combustion of diverse waste materials in household stoves or small industrial boilers and is predominantly observable during the spring and early summer months, with an increased contribution in the autumn and winter periods. The relative monthly contribution of this source reaches up to 5.5 $\mu\text{g}/\text{m}^3$ or 19.7 %, while the annual contribution is 9 %.

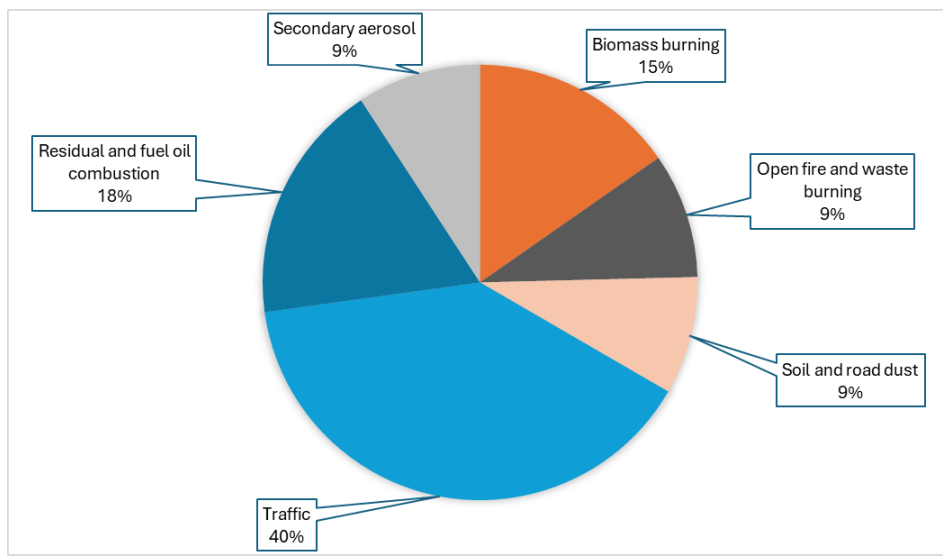


Figure 40. Relative annual contribution of PM 2.5 sources at Struga

Secondary aerosols are particles that are not directly emitted but are generated by various chemical reactions in the atmosphere, influenced by sunlight, ozone, and humidity, ultimately resulting in the formation of "secondary aerosols." Secondary aerosols demonstrate their greatest contribution during the coldest and warmest months, perhaps linked to elevated quantities of gaseous precursors in winter and photochemical reactions resulting from high temperatures in summer. The annual relative contribution of secondary aerosols was 9% of the total particle mass (PM2.5), with monthly contributions displaying significant variability, ranging from 0.3 % to 20.4 %.

6. Conclusions and recommendations

The Struga urban area is not covered with the national monitoring network, and no other program has monitored ambient air quality there, so there is no historical data. However, due to poor waste management practices and frequent landfill fires, ambient air quality has become a recognized and openly discussed issue.

The AMBICON Laboratory conducted this Source Apportionment Study to gather information on pollution sources and their contributions to ambient air pollution in Struga. The activities followed the strict guidelines in the European handbook on air pollution source apportionment using receptor models (Revised edition 2019, JRC) and included a year-long program for collecting and analyzing air samples, which helped create a complex model to identify pollution sources. The sampling program started on March 4, 2023, and until the end of March 2024, 194 samples were collected, with a 24-hour sample being taken every other day. The sampling process was executed in strict compliance with the standard gravimetric measurement method for determining the mass concentration of PM10/PM2.5 suspended particulate matter (EN 12341:2014). Energy dispersive X-ray fluorescence (ED-XRF) was used to analyze the elements, an optical transmissometer measured the amount of elemental carbon, and spectrophotometry helped identify water-soluble ions.

The daily average PM2.5 concentrations measured at the Struga monitoring site exhibit significant daily and seasonal variations, exceeding all European Union limits, targets, and thresholds for human health protection. Concentrations measured ranged from a minimum of $3.8 \mu\text{g}/\text{m}^3$ to a maximum of $117.8 \mu\text{g}/\text{m}^3$, resulting in an average annual value of $30.3 \mu\text{g}/\text{m}^3$, which exceeds the annual threshold limit value of $25 \mu\text{g}/\text{m}^3$ by 21%. The percentage of days surpassing the annual limit for PM 2.5 ($25 \mu\text{g}/\text{m}^3$) was an alarming 52.5% (94 out of 180 valid daily readings).

Surprisingly, there are no significant differences between the average concentrations during the warm and cold months. The average concentration during the heating season is $29.7 \mu\text{g}/\text{m}^3$, which is slightly (4 %) lower than the average in the spring and summer months, when the average value is $30.8 \mu\text{g}/\text{m}^3$.

Modelled data, show that there is no apparent variation in particulate matter concentration by day of the week or time of day during the spring, summer, or even autumn. On the opposite side, although there are no significant differences between the days of the week, during the winter there are expressed daily variations with distinct peaks in particulate matter levels at specific times of the day (early morning and late evening). This pattern is often influenced by an interaction of meteorological factors, anthropogenic activities, and local emissions, and is predominantly attributed to the increased utilization of woodstoves and other solid fuel heating means, which discharge substantial quantities of particulate matter into the atmosphere.

Polar plots generated for the Struga area demonstrate concentration variations influenced from local meteorological conditions, notably indicating that elevated PM concentrations are exclusively observed during the winter season and are predominantly linked to low wind speeds (1 to 2 m/s), from all directions, primarily east and northeast. Non-parametric wind regression (NWR) plots also indicates that most of the pollution is associated with weak winds blowing from the north and northeast, suggesting that the pollution is local, or from nearby settlements (Misleshevo, Moriosta, Draslajica and Vranishta) and the main roads. Given that this direction also corresponds with the urban area of the city, it implies that the sources of pollution are also within the city limits.

Using the data from measurements and modelling exercise, contribution of each source to total particulate mass (PM 2.5) was calculated. The major sources identified for Struga include

biomass burning, open fire and waste burning, traffic, secondary aerosols, road and soil dust, and fuel and residual oil burning.

On annual level, traffic represents the primary air pollution source, demonstrating a steady contribution throughout the year, with a notable increase during the summer and fall months. The annual relative contribution of traffic constituted 40 % of the total particulate mass (PM 2.5), with monthly relative contributions varying up to 55.7 %.

Fuel and residual oil contribute from 1.4 and 7.9 $\mu\text{g}/\text{m}^3$ to total particulate mass. This source occurs consistent over the year. Annual relative contribution of fuel and residual oil combustion accounted for 18 % of the total particulate mass (PM 2.5) mass. Relative monthly contribution ranged from 5.2 to 40 %.

Biomass burning was a significant source in the municipality of Struga during the winter months, with the biggest contribution to total particle mass occurring in November, December, January, February, and March, while having minimal impact during the summer months. The average monthly contribution of biomass burning over the winter season is up to 15.4 $\mu\text{g}/\text{m}^3$. The relative contributions (%) of biomass burning to total particle mass demonstrate significant seasonal variability, with this source accounting up to 50 % during winter months, and although entirely seasonal, biomass burning accounts for a significant annual relative contribution of 15%.

It is evident that, due to its complexity, air pollution cannot be addressed by reducing emissions from a single source, but rather by reducing emissions from all sources simultaneously. Furthermore, most air pollution problems cannot be addressed with immediate or quick steps; consequently, a continuous and comprehensive approach, supported by systematic measures, is required, with outcomes expected in the foreseeable future, based on the positive experiences of other countries.

Utilizing experiences and examples from communities that have achieved noticeable improvements is an effective strategy. In response to this urgent concern, a committed UNDP project team has compiled a comprehensive dataset highlighting innovative air protection measures worldwide. This program aims to map global air protection solutions, providing access to a diverse range of beneficial activities, policies, or strategies at local and national levels, while showcasing exemplary cases in the battle against air pollution [53].

The Polish city of Krakow, which is regarded as having some of the worst air quality in Europe, is also an excellent example. Today's scenario is entirely different thanks to the city's leadership and citizens' tenacious actions. Krakow has greatly lowered the concentrations of all pollutants and complies with today's ambient air quality standards thanks to a comprehensive program to enhance air quality that offers inhabitants both practical and financial assistance to upgrade their home heating systems [54].

Consequently, the formulation of targeted and comprehensive plans for air quality management, based on contemporary scientific evidence, along with a robust political commitment to their execution, is imperative.

Lessons learned

Lesson No. 1	Solutions available
<p>Traffic-related air pollution can be a significant source, contributing consistently throughout the year, with a noticeable increase during the summer months. Struga, being a popular tourist destination, attracts large numbers of visitors primarily in June, July, and August. Since tourists typically arrive by car, it is expected that traffic will increase during this period, leading to higher levels of pollution. The annual relative contribution of transportation accounts for 40% of the total particle mass.</p>	<p>Measures aimed at urban planning, raising awareness, and implementing clean vehicle policies and incentives form the foundation for a sustainable reduction in traffic pollution. However, these approaches often entail significant costs and require long-term commitments. In contrast, certain measures, such as traffic restrictions (including low-emission zones and car-free areas) and enhancements to public and active transportation, can be executed more quickly and effectively reduce traffic pollution. Successful strategies typically encompass a combination of actions working together. Examples include a well-expanded and improved public transport network that features frequent, reliable, and environmentally friendly buses, along with safe bike lanes, bike-sharing initiatives, park-and-ride systems located at the outskirts of the city, and congestion charges implemented in the city center, are some of the solutions that have proven effective worldwide.</p>
<p>Lesson No. 2</p> <p>The widespread use of fuel oil boilers in public buildings and woodstoves in homes as main heating sources is one of the key reasons for high levels of fine particulate matter (PM2.5) in many cities across the country.</p>	<p>Although complex, there are numerous successful examples of updating public buildings and house heating systems to provide more sustainable options for heating. In densely populated areas, district or local heating systems may be the best option. In individual homes, replacing old wood stoves with exceptionally effective "air-to-air" or "air-to-water" heat pumps or natural gas boilers (if available) can virtually eliminate particulate emissions from this sector, greatly improving overall air quality and lowering the frequency of high pollution episodes in our cities. Small-scale electrical and thermal energy production plants, when combined with cost-effective heat pumps, can provide an economically viable solution to the current situation and pave the way for long-term success. Nevertheless, the success of any future initiatives is based upon the development of focused and broad plans, as well as financial and practical support, strong political commitment, and public support.</p>

References

1. Struga Municipality Air Quality Improvement Plan for 2023-2027, Tehnolab, 2024)
2. Available at the link: <https://en-gb.topographic-map.com/map-lx6q4s/Struga/>
3. Climate maps, UHMR, 2020
4. MaxStat Database, available at the link:
<https://makstat.stat.gov.mk/PXWeb/pxweb/mk/MakStat/>
5. Available at the link: <https://arhiva.moepp.gov.mk/wp-content/uploads/2014/10/A-Nacrt-Integrirane-eko-dozvola-ILINDEN-STRUGA.pdf>
6. Available at the link: <https://www.struga.gov.mk/mk/>
7. Chen, K., Zhou, L., Chen, X., Bi, J., & Kinney, P. L. (2017). Acute effect of ozone exposure on daily mortality in seven cities of jiangsu province, china: no clear evidence for threshold. *Environmental Research*, 155, 235-241. <https://doi.org/10.1016/j.envres.2017.02.009>
8. Frei, M., Kohno, Y., Wissuwa, M., Makkar, H., & Becker, K. (2011). Negative effects of tropospheric ozone on the feed value of rice straw are mitigated by an ozone tolerance qtl. *Global Change Biology*, 17(7), 2319-2329. <https://doi.org/10.1111/j.1365-2486.2010.02379.x>
9. Davis, D. D. and Decoteau, D. R. (2018). A review: effect of ozone on milkweeds (*asclepias* spp.) in usa and potential implications for monarch butterflies. *Journal of Agriculture and Environmental Sciences*, 7(2). <https://doi.org/10.15640/jaes.v7n2a16>
10. Available at the link: <https://source-apportionment.jrc.ec.europa.eu/Specieurope/index.aspx>
11. EMEP/EEA air pollutant emission inventory guidebook 2019, EEA Report 13/2019, available at the link: <https://www.eea.europa.eu/en/analysis/publications/emeep-eea-guidebook-2019>
12. Pernigotti, D., Belis, C.A., Spanó, L., 2016. SPECIEUROPE: The European data base for PM source profiles. *Atmospheric Pollution Research*, 7 (2), pp. 307-314. DOI: 10.1016/j.apr.2015.10.007
13. Rigaku NEX CG, website: <https://www.rigaku.com/products/edxrf/nexcg>
14. Standard Operating Procedure for PM2.5 Cation Analysis, revision 7, August 2009, Environmental and Industrial Sciences Division RTI International, Research Triangle Park, North Carolina
15. Guo, H., Gu, X., Ma, G., Shi, S., Wang, W., Zuo, X., ... & Zhang, X. (2019). Spatial and temporal variations of air quality and six air pollutants in China during 2015–2017. *Scientific Reports*, 9(1). <https://doi.org/10.1038/s41598-019-50655-6>
16. Thabethe, N. D., Makonese, T., Masekameni, D., & Brouwer, D. (2024). Diurnal and seasonal variations of particulate matter (PM 2.5) at a tailing storage facility and nearby community. <https://doi.org/10.21203/rs.3.rs-3875400/v1>
17. Yorkor, B., Leton, T. G., & Ugbebor, J. N. (2021). Analysis of temporal variations of air pollutant concentrations in ogoni area, niger delta region, nigeria. *Asian Journal of Environment & Ecology*, 63-73. <https://doi.org/10.9734/ajee/2021/v16i430260>
18. Onanuga, K., Daniel, V., Mustapha, A., & Maitera, O. (2024). Seasonal variations assessment of air pollutants of communities in the vicinity of scrap metal recycling industries in ogijo, shagamu south lga, ogun state, sw nigeria. *Asian Journal of Applied Chemistry Research*, 15(1), 37-47.
19. Liu, X., Wei, Y., Liu, X., Zu, L., Wang, B., Wang, S., ... & Zhu, R. (2022). Effects of winter heating on urban black carbon: characteristics, sources and its correlation with meteorological factors. *Atmosphere*, 13(7), 1071. <https://doi.org/10.3390/atmos13071071>

20. Putaud, J.P., Van Dingenen, R., Alaustey, A., Bauer, H., Birmili, W., et al., 2010. A European aerosol phenomenology – 3: physical and chemical characteristics of particulate matter from 60 rural, urban, and kerbside sites across Europe. *Atmos. Environ.* 44, 1308–1320.
21. Source Apportionment Study for Skopje urban area – identification of main sources of ambient air pollution, AMBICON Lab, Goce Delcev University, Stip, North Macedonia
22. Norris, G., R. Duvall, S. Brown, AND S. Bai. EPA Positive Matrix Factorization (PMF) 5.0 Fundamentals and User Guide. U.S. Environmental Protection Agency, Washington, DC, EPA/600/R-14/108 (NTIS PB2015-105147), 2014.
23. Lee E, Chan C.K., Paatero P., (1999). Application of positive matrix factorization in source apportionment of particulate pollutants in Hong Kong. *Atmospheric Environment*, 33, 3201–3212.
24. Polissar A.V., Hopke P.K., Paatero P., Kaufmann Y.J., Hall D.K., Bodhaine B.A., Dutton E.G., Harris J.M., (1999). The aerosol at Barrow, Alaska: long-term trends and source locations. *Atmospheric Environment*, 33, 2441–2458.
25. Sukon Aimanant & Paul J. Ziemann (2013) Development of Spectrophotometric Methods for the Analysis of Functional Groups in Oxidized Organic Aerosol, *Aerosol Science and Technology*, 47:6, 581-591, DOI: 10.1080/02786826.2013.773579
26. Xie Y., Berkowitz C.M., (2006). The use of positive matrix factorization with conditional probability functions in air quality studies: an application to hydrocarbon emissions in Houston, Texas. *Atmospheric Environment*, 40, 3070–3091.
27. Begum B.A., Kim E., Biswas S.K., Hopke P.K., (2004). Investigation of sources of atmospheric aerosol at urban and semi-urban areas in Bangladesh. *Atmospheric Environment*, 38, 3025–3038.
28. Bzdusek P.A., Christensen E.R., Lee C.M., Pakadeesusuk U., Freedman D.C., (2006). PCB congeners and dechlorination in sediments of Lake Hartwell, South Carolina, determined from cores collected in 1987 and 1988. *Environmental Science and Technology*, 40, 109–119.
29. Singh K.P., Malik A., Singh V.K., Sinha S., (2006). Multi-way data analysis of soils irrigated with wastewater. A case study. *Chemometrics and Intelligent Laboratory Systems*, 83, 1-12.
30. Soonthornnonda P., Christensen E.R., (2008). Source apportionment of pollutants and flows of combined sewer wastewater. *Water Research*, 42, 1989–1998.
31. Hopke P.K., (2003). Recent developments in receptor modeling. *Journal of chemometrics*, 17, 255–265.
32. Belis C.A., Favez O., Mircea M., Diapouli E., Manousakas M-I., Vratolis S., Gilardoni S., Paglione M., Decesari S., Mocnik G., Mooibroek D., Salvador P., Takahama S., Vecchi R., Paatero P., European guide on air pollution source apportionment with receptor models - Revised version 2019, EUR 29816 EN, Publications Office of the European Union, Luxembourg, 2019, ISBN 978-92-76-09001-4, doi:10.2760/439106, JRC117306.
33. Polissar, A. V., Hopke, P. K., & Poirot, R. L. (2001). Atmospheric aerosol over Vermont: chemical composition and sources. *Environmental science & technology*, 35(23), 4604–4621. <https://doi.org/10.1021/es0105865>
34. Mirakovski, D., Zendelska, A., Boev, B. et al. Evaluation of PM2.5 Sources in Skopje Urban Area Using Positive Matrix Factorization. *Environ Model Assess* 29, 1–14 (2024). <https://doi.org/10.1007/s10666-024-09961-1>
35. H. Simon, L. Beck, P.V. Bhate, F. Divita, Y. Hsu, D. Luecken, J.D. Mobley, G.A. Pouliot, A. Reff, G. Sarwar, M. Strum, The development and uses of EPA's SPECIATE database, *Atmos. Pollut. Res.* (2010), pp. 196-206, 10.5094/APR.2010.026

36. Zhang, X., Hecobian, A., Zheng, M., Frank, N. H., and Weber, R. J.: Biomass burning impact on PM_{2.5} over the southeastern US during 2007: integrating chemically speciated FRM filter measurements, MODIS fire counts and PMF analysis, *Atmos. Chem. Phys.*, 10, 6839-6853, 10.5194/acp-10-6839-2010, 2010.
37. Lee, S., Liu, W., Wang, Y., Russell, A. G., and Edgerton, 948 E. S.: Source apportionment of PM 2.5: Comparing PMF and CMB results for four ambient monitoring sites in the southeastern United States, *Atmos. Environ.*, 42, 4126-4137, 2008.
38. Duvall, R. M., Majestic, B. J., Shafer, M. M., Chuang, P. Y., Simoneit, 846 B. R. T., and Schauer, J. J.: The water-soluble fraction of carbon, sulfur, and crustal elements in Asian aerosols and Asian soils, *Atmos. Environ.*, 42, 5872-5884, <https://doi.org/10.1016/j.atmosenv.2008.03.028>, 2008.
39. Almeida et al. (2020) Ambient particulate matter source apportionment using receptor modelling in European and Central Asia urban areas, *Environmental Pollution*, Volume 266, Part 3, <https://doi.org/10.1016/j.envpol.2020.115199>
40. Sun, Y., Zhuang, G., Tang, A., Wang, Y., and An, Z.: Chemical Characteristics of PM_{2.5} and PM₁₀ in Haze-Fog Episodes in Beijing, *Environ. Sci. Technol.*, 40, 3148-3155, 10.1021/es051533g, 2006.
41. Zhou, Y., Zheng, N., Luo, L., Zhao, J., Qu, L., Guan, H., Xiao, H., Zhang, Z., Tian, J., and Xiao, H.: Biomass burning related ammonia emissions promoted a self-amplifying loop in the urban environment in Kunming (SW China), *Atmos. Environ.*, 118138, <https://doi.org/10.1016/j.atmosenv.2020.118138>, 2020.
42. Paulot, F., Paynter, D., Ginoux, P., Naik, V., Whitburn, S., Van Damme, M., Clarisse, L., Coheur, P. F., and Horowitz, L. W.: Gas-aerosol partitioning of ammonia in biomass burning plumes: Implications for the interpretation of spaceborne observations of ammonia and the radiative forcing of ammonium nitrate, 44, 8084-8093, <https://doi.org/10.1002/2017GL074215>, 2017.
43. Pant, P., and Harrison, R. M.(2013): Estimation of the contribution of road traffic emissions to particulate matter concentrations from field measurements: A review, *Atmos. Environ.*, 77, 78-97, <https://doi.org/10.1016/j.atmosenv.2013.04.028>.
44. Pant, P., and Harrison, R. M.(2012): Critical review of receptor modelling for particulate matter: a case study of India, *Atmos. Environ.*, 49, 1-12.
45. Grigoratos, T., and Martini, G (2019): Brake wear particle emissions: a review, *Environ. Sci. Pollut. Res.*, 22, 2491-2504, 10.1007/s11356-014-3696-8, 2015.
46. Piscitello, A., Bianco, C., Casasso, A., and Sethi, R.: Non-exhaust traffic emissions: Sources, characterization, and mitigation measures, *Sci. Total Environ.*, 766, 144440, <https://doi.org/10.1016/j.scitotenv.2020.144440>, 2021.
47. Smichowski, P., Gómez, D., Fazzoli, C., and Caroli, S.: Traffic-Related Elements in Airborne Particulate Matter, *Applied Spectroscopy Reviews*, 43, 23-49, 10.1080/05704920701645886, 2007.
48. Duong, T. T. T., and Lee, B.-K.: Determining contamination level of heavy metals in road dust from busy traffic areas with different characteristics, *J. Environ. Manage.*, 92, 554-562, <https://doi.org/10.1016/j.jenvman.2010.09.010>, 2011.
49. Liao, H.T., Chou, C.C.K., Chow, J.C., Watson, J.G., Hopke, P.K., Wu, C.F., (2015). Source and risk apportionment of selectes VOCs and PM_{2.5} species using partially constrained receptor models with multiple time resolution data. *Environ. Pollut.* 205, 121-130.
50. Yu, L., Wang, G., Zhang, R., Zhang, L., Song, Y., Wu, B., Li, X., An, K., and Chu, J. (2013): Characterization and source apportionment of PM_{2.5} in an urban environment in Beijing, *Aerosol Air Qual. Res.*, 13, 574-583, 10.4209/aaqr.2012.07.0192.

51. Zhang, Y., Sun, J., Zhang, X., Shen, X., Wang, T., and Qin, M. (2013): Seasonal characterization of components and size distributions for submicron aerosols in Beijing, *Sci. China Earth Sci.*, 56, 890- 900, 10.1007/s11430-012-4515-z.
52. Paul M Lemieux, Christopher C Lutes, Dawn A Santoianni (2004): Emissions of organic air toxics from open burning: a comprehensive review, *Progress in Energy and Combustion Science*, 30, 1, <https://doi.org/10.1016/j.pecs.2003.08.001>
53. Available at the link: <https://www.undp.org/north-macedonia/blog/scaling-solutions-leveraging-open-data-tackle-air-pollution>
54. Available at the link: https://environment.ec.europa.eu/topics/urban-environment/inspiration/krakow-air-protection_en
55. Guidelines for drafting air quality improvement plan. <http://air.moepp.gov.mk/wp-content/uploads/2017/04/Pravilnik-plan-za-podobravanje-na-kvalitetot-na-vozduhot.pdf>